ChromGene: Gene-Based Modeling of Epigenomic Data

Artur Jaroszewicz[1,2] and Jason Ernst[1,2,3,4,5,6,7*]

[1] Bioinformatics Interdepartmental Program, [2] Department of Biological Chemistry, [3] Eli and Edythe Broad Center of Regenerative Medicine and Stem Cell Research, [4] Computer Science Department, [5] Computational Medicine Department, [6] Jonsson Comprehensive Cancer Center and [7] Molecular Biology Institute, University of California, Los Angeles, Los Angeles, CA 90095, USA

*To whom correspondence should be addressed.

Contact email (jason.ernst@ucla.edu)

Abstract

Background: Computational approaches have been developed and broadly used for annotating epigenomes on a per position basis by modeling combinatorial and spatial patterns within epigenomic data. However, such annotations are less suitable for gene-based analyses, in which a single annotation for each gene is desired.

Results: To address this, we developed ChromGene to annotate genes based on the combinatorial and spatial patterns of multiple epigenomic marks across the gene body and flanking regions. Specifically, ChromGene models the epigenomics maps using a mixture of hidden Markov models learned *de novo*. Using ChromGene, we generated annotations for the human protein-coding genes for over 100 cell and tissue types. We characterize the different mixtures and their associated gene sets in terms of gene expression, constraint, and other gene annotations. We also characterize variation in ChromGene gene annotations across cell and tissue types.

Conclusions: We expect that the ChromGene method and provided annotations will be a useful resource for gene based epigenomic analyses.

Keywords: Chromatin, machine learning, hidden Markov models, histone modifications, epigenomics

Introduction

Genome-wide maps of epigenomic marks such as histone modifications from Chromatin Immunoprecipitation followed by high-throughput sequencing (ChIP-seq) experiments and chromatin accessibility from DNase-seq or ATAC-seq experiments provide valuable information for annotating the genome in a cell type specific manner [1–7]. Notably, a number of approaches have been developed for annotating the genome into 'chromatin states' based on the combinatorial and spatial patterns of epigenomic marks inferred de novo from the data. These different 'chromatin states' can correspond to different classes of genomic elements, including enhancers, promoters, and repressive regions [8–10]. Annotations from these methods have been used for a diverse range of applications including understanding gene regulation and genetic variants associated with disease [2, 11, 12].

While some applications rely on per-position chromatin-state annotations across the genome, other applications require gene-based annotations. Notably, transcriptomic data is predominantly used for gene-based analyses [13–15]. However, taking full advantage of epigenomic data to generate gene-based annotations is less straightforward than for per-position annotations. The challenge with gene-based annotations is that the combination of epigenomic marks will vary along a gene in a position dependent manner. Furthermore, protein-coding genes can have vastly different gene lengths ranging from a few hundred base pairs to over 2Mb (median

30kb) [16]. One strategy for gene-based annotations is to focus on the chromatin state at the transcription start site (TSS) [8, 17]. While such an approach is largely independent of varying gene lengths, it ignores potentially important information throughout the gene body. A simple alternative strategy would be based on averaging each mark's signal across the entire gene [18]. However, such an approach loses information about which marks co-occur along the gene, and has the potential to be heavily confounded by gene length.

Another strategy has been to partition genes into regions and cluster the genes based on mark signal in those regions. For example, one study partitioned genes into five regions: the 500bp region upstream of the TSS, the 500bp region downstream of the TSS, and the remaining gene body into equal thirds. The study then averaged the per-mark signal within each region and applied the *k*-medoids algorithm to cluster [19]. However, such an approach is dependent on the specific choices of the partition and loses information due to averaging within each partition.

Other work has solved related but different problems. EPIGENE used hidden Markov models (HMMs) to identify transcription units [20], but is not designed for clustering them. Hierarchical or multi-tiered HMMs have been proposed to capture broader domains, but are not designed to provide a single annotation per gene in a cell or tissue type [21–23]. (Note: Henceforth, we will use the term "cell type" instead of "cell or tissue type" for ease of presentation). EpiAlign was proposed to align chromatin states between two regions, such as genes, and identify corresponding regions [24], but is also not designed for *de novo* gene based annotations.

There is thus a need for a principled, model-based method that can be used to generate *de novo* annotations of known genes based on the combinatorial and spatial information in datasets of multiple epigenomic marks. To address this, we introduce ChromGene. ChromGene uses a mixture of HMMs to model the combinatorial and spatial information of epigenomics maps

throughout a gene body and flanking regions. Furthermore, ChromGene can learn a common model across multiple cell types and use it to generate per-gene annotations for each.

Here, we apply ChromGene to ChIP-seq data of histone marks and DNase-seq data from over 100 cell types and produce per-gene annotations for each one. We describe these annotations with respect to their mark emissions and relate them to gene expression data and other external data, including genes with high probability of loss-of-function (LoF) intolerance (pLI) [25]. We show that ChromGene annotations show better agreement with gene expression and stronger Gene Ontology (GO) and cancer gene set enrichments than other methods. We expect the ChromGene annotations we have produced will be a resource for gene-based epigenomic analyses, and that the methodological approach will be useful for applications to other epigenomic data.

Results

Overview of ChromGene method

ChromGene models the set of epigenomic data across genes with a mixture of HMMs (**Fig. 1**) by extending ChromHMM [9] (**Methods**, **Supp. Methods**, **Supp. Fig. 1**). The set of epigenomic data for each gene and its flanking region is binarized at fixed-width intervals, indicating observations of each epigenomic mark, before being input to ChromGene. The data for a given gene in a cell type is modeled as being generated by one of M HMMs. Each individual HMM has S hidden states. The emission distribution is modeled with a product of independent Bernoulli random variables following ChromHMM. There are no constraints on allowed transitions between states of one HMM, but there are no allowed transitions between states of different HMMs. There is also an initial state distribution, or the probability of seeing a state first at the beginning of the gene flanking region, over states of the HMMs. The prior probability that a gene belongs to a mixture

corresponds to the sum of initial state probabilities of the states of the mixture. For given values of *M* and *S*, the parameters of the model are learned from the data by an expectation-maximization approach aiming to maximize the likelihood of the model parameters. Once a model is trained, ChromGene computes the posterior probability of each of *M* mixtures generating each gene's data in a given cell type. For that cell type, each gene is then assigned to the mixture for which it has the greatest posterior probability.

To model data from multiple cell types, ChromGene can be applied analogously to the 'concatenated' approach of ChromHMM [2, 26], which gives cell type specific assignments based on a common model. To do this, ChromGene treats the same gene in different cell types as if it were different genes in the same cell type when learning the model. Using this common model, a gene is independently assigned a mixture assignment for each cell type.

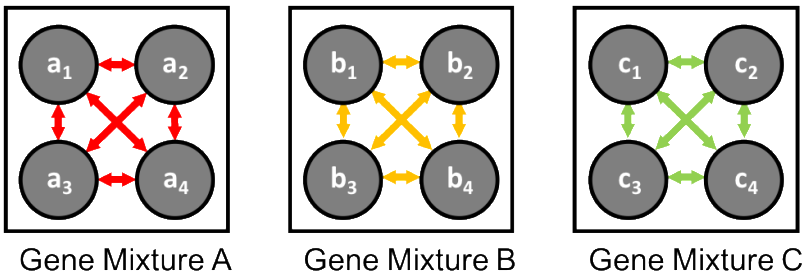

Figure 1: The ChromGene model

Each gene is assumed to be generated by one of *M* mixtures (*A*, *B*, *C*, …), each of which is defined by *S* states. The states within a mixture have learned probabilities of transition between them, but transitions between states in different mixtures are disallowed. Each state has a separate emission probability for each input mark, corresponding to the parameter of a Bernoulli random variable, and the probability of a set of observed marks is modeled using a product of those Bernoulli random variables.

ChromGene generates distinct gene-level chromatin annotations

We applied ChromGene to imputed data for ten histone modifications (H3K9me3, H3K36me3, H4K20me1, H3K79me2, H3K4me1, H3K27ac, H3K9ac, H3K4me3, H3K4me2, and H3K27me3), histone variant H2A.Z, and DNase-seq data from 127 cell types, binarized at 200bp resolution [1, 27] across 19,919 protein coding genes [16] using the 'concatenated' approach. We focused our analysis on a model with *M=12* mixtures and *S=3* states per mixture to balance model interpretability while capturing biologically relevant state distinctions.

Based on the emission parameters of the model (**Fig. 2a**), along with the relationship of the mixtures to external data not used in model learning (discussed below), we gave each mixture a candidate interpretation (**Fig. 3**, **Supp. Table 1**). Eight of the mixtures ('strong_trans_enh', 'strong_trans', 'trans_enh', 'trans_cons', 'trans_K36me3', 'trans_K79me2', 'weak_trans_enh', and 'znf') had at least one state with H3K36me3 or H3K79me2, both transcription associated histone modifications, present at >31% of positions. All of these mixtures had at least one state associated with high frequency of promoter-associated H3K4me3 or H3K4me2 (>73%) and limited detection of the repressive mark H3K27me3 (<15%). In four of these mixtures ('strong_trans_enh', 'strong_trans', 'trans_enh', and 'trans_cons'), all three of its states had a high-frequency (>28%) for at least one mark. In contrast, the mixtures 'trans_K36me3', 'trans_K79me2', 'weak_trans_enh', and 'znf' all had one state with low frequency of all marks (<7%). Mixture 'znf' is notable in that the H3K36me3 co-occurs with the repressive mark H3K9me3. This mixture shows 11-fold enrichment for Zinc finger named (ZNF) genes on average, consistent with previous findings for this combination of marks from per-chromatin state analyses [8, 27]. Three of the mixtures ('strong_trans_enh', 'trans_enh', and 'weak_trans_enh') had a state with H3K4me1 being the mark with the greatest frequency (>78% in all cases) and limited H3K4me3 (<5% of positions), consistent with previously described putative enhancers [8, 27, 28].

Mixtures ‘trans_K36me3’ and ‘trans_K79me2’ were both associated with a state containing high frequency for active marks typically found at promoters or enhancers, a state with a low frequency of all marks, and a state dominated by H3K36me3 and H3K79me2, respectively.

The four remaining mixtures (‘poised’, ‘bivalent’, ‘low’, ‘quiescent’) lacked any state with the transcription associated marks, H3K36me3 or H3K79me2, at a high frequency (<12% for all states). Mixtures ‘poised’ and ‘bivalent’ had states with high frequencies of other marks. Notably, the ‘bivalent’ mixture had a state associated with the high presence of the repressive mark H3K27me3 in combination with H3K4me1/2/3, along with another state associated with H3K27me3 alone. Mixture ‘low’ only had one of its states associated with moderate levels of histone marks, which were not associated with transcription. No state of the ‘quiescent’ mixture had any detected modifications (all emissions <1%).

The assignments for all 127 cell types across 19,919 genes are provided as a Supplementary Data file and available at [https://github.com/ernstlab/ChromGene/]. To visualize the assignments, we sampled 2000 genes and clustered them based on assignment to ChromGene mixtures across all cell types (**Fig. 2b**).

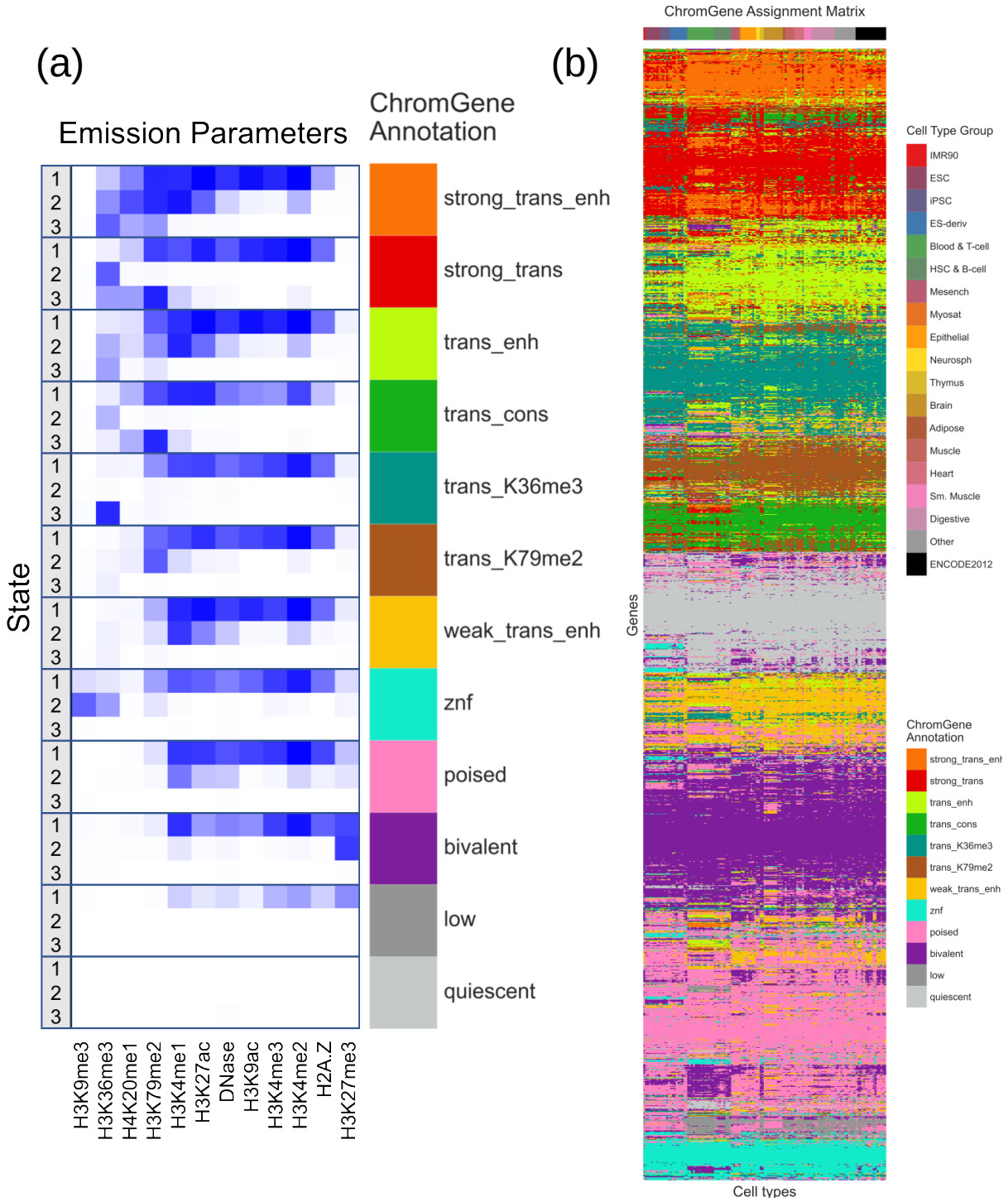

Figure 2: The emissions parameters and assignment of genes to ChromGene mixtures.

(a) Heatmap of emission parameters with blue corresponding to a higher probability and white a lower. The ChromGene mixtures are labeled on the right and the states within each mixture are labeled on the left. Mixtures are ordered from top to bottom by decreasing expression, and states within each

mixture are ordered by decreasing enrichment at the gene TSS. Marks are ordered from left to right as previously done [27]. Transition probabilities are pictured in **Supp. Fig. 2**; per-state emission probabilities and enrichments, along with transition probabilities, are also reported (**Supp. Table 1**).

(b) Graphical representation of the ChromGene assignment matrix. Columns correspond to cell types, which are ordered as previously done [1], and their tissue group is indicated by the top colorbar and top legend. Rows correspond to 2000 subsampled genes (approximately 10% of all genes). Rows were ordered by hierarchical clustering (**Supp. Methods**). Each cell is colored by ChromGene annotation for the corresponding cell type and gene (lower legend).

	Mnemonic	Description	Overall Percentage	Median Expression (RPKM)	Median Length (kb)	Percentage of High-pLI Genes (pLI > 0.9)	Cell Type Specificity	Housekeeping Gene Enrichment	Constitutive Unexpressed Gene Enrichment	Constitutive Expressed Gene Enrichment	Olfactory Gene Enrichment	ZNF Gene Enrichment
	strong_trans_enh	Shorter, highest expressed genes, strong H3K4me1/H4K20me1 initiation associated; second highest pLI	5.60	33.94	15.03	36.13	0.31	2.31	0.02	1.98	0.00	0.38
	strong_trans	Strong H3K36me3 state and strong H3K79me2 state - second highest expressed, and third highest pLI genes	10.50	18.24	24.03	30.61	0.22	3.05	0.01	2.62	0.00	0.81
	trans_enh	Active promoter state, some H3K79me2 with enhancer marks and some H3K36me3, third highest expressed, relatively short genes	8.96	13.89	14.58	12.96	0.41	1.65	0.05	1.69	0.00	0.70
	trans_cons	Strong H3K79me2 and weaker H3K36me3, second longest genes, fourth highest expressed genes, highest pLI	4.49	12.73	88.38	46.84	0.30	2.00	0.03	2.32	0.00	0.55
	trans_K36me3	Transcribed with strong H3K36me3, but weak H3K79me2	10.78	6.78	27.13	11.53	0.24	1.45	0.13	1.49	0.02	1.31
	trans_K79me2	Transcribed with strong H3K79me2 state, but weak H3K36me3	7.34	6.09	55.38	19.50	0.32	1.26	0.13	1.71	0.01	0.46
	weak_trans_enh	Enhancer state, with weaker transcription, more intermediate expression levels	7.13	4.29	33.54	11.01	0.49	0.46	0.29	0.50	0.05	0.39
	znf	ZNF genes	4.75	0.94	33.33	4.05	0.23	0.33	1.64	0.29	1.92	10.96
	poised	Poised genes - lack transcription marks, has promoter/enhancer marks, limited repressive marks	16.39	0.35	41.62	10.16	0.33	0.08	1.04	0.09	0.17	0.27
	bivalent	Strong K27me3/bivalent genes; low expression; development genes	14.13	0.04	14.02	11.29	0.23	0.03	1.43	0.02	0.86	0.17
	low	Weak K27me3, low signal of other marks, low expression, longest genes	1.85	0.02	114.92	16.27	0.43	0.00	1.42	0.05	0.24	0.27
	quiescent	Quiescent - unmarked; low expression; olfactory genes; very low pLI; short genes	8.08	0.00	3.52	0.77	0.16	0.01	5.83	0.05	9.20	0.12

Figure 3: Brief description of each ChromGene annotation

Each row after the header row corresponds to a ChromGene annotation. The columns are as follows: Color: color used for ChromGene annotation, Mnemonic: abbreviated name used for annotation, Description: description of each ChromGene annotation based on mark emissions, expression, length, pLI, and other enrichments. Subsequent columns describe summary statistics of ChromGene annotations: 'Overall Percentage, 'Median Expression' (RPKM) and 'Median Length' (kb) of genes assigned to annotation; 'Percentage of High-pLI Genes (pLI > 0.9)' – percentage of genes assigned to annotation with > 0.9 pLI (probability of Loss of function Intolerance); 'Cell Type Specificity' – metric of variability of annotation across cell types; 'Housekeeping Gene Enrichment', 'Constitutive Unexpressed Gene Enrichment', 'Constitutive Expressed Gene Enrichment', 'Olfactory Gene Enrichment', 'ZNF Gene Enrichment' – fold enrichment of gene category within annotation compared to 'Overall Percentage'.

ChromGene relationship with gene expression levels

We first investigated how the ChromGene annotation of a gene relates to its expression level. We compared ChromGene annotations to matched gene expression data for 56 cell types [1] (Methods). We separated cell type-gene combinations by their ChromGene annotation and analyzed the distribution of gene expression values (RPKM) for each annotation. We observed that genes assigned to different annotations had varying levels of expression (**Fig. 4**). The two annotations with the highest expression ('strong_trans_enh' and 'strong_trans') both had states with a high frequency of H3K36me3 and H3K79me2. The four annotations with the lowest expression ('poised', 'bivalent', 'low' and 'quiescent') each had a median RPKM of less than 1. Notably, the 'quiescent' and 'bivalent' mixtures had a large overlap in distribution of gene expression levels, despite the lack of the former with any state with substantial frequency of histone modifications, and the association of the latter with histone modifications in multiple states. This

highlights how ChromGene provides additional information about genes not captured by gene expression.

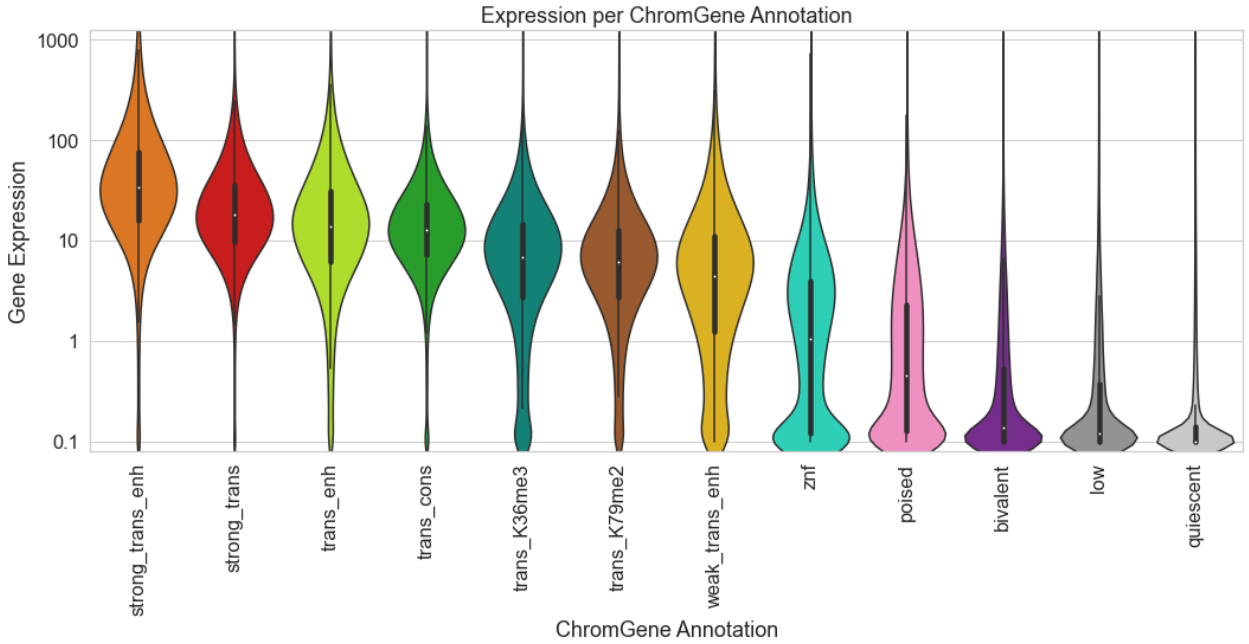

Figure 4: Gene expression distribution of ChromGene annotations

The gene expression distribution for each ChromGene annotation across 56 cell types. Gene expression values are in RPKM after a pseudocount of 0.1 is added to each gene expression value, and then $\log_{10}$ transformed for visualization.

For each ChromGene annotation, we also determined how consistent average gene expression levels were across cell types. Specifically, for each annotation and cell type, we calculated the median $\log_{10}$(RPKM + 0.1) expression and analyzed the medians as a function of annotation (**Supp. Fig. 3**). We then calculated the mean within-annotation variance across cell types (0.026) and the total variance of the computed medians (0.783). We found that median expression variance within annotations were significantly smaller than across annotations (p-value

$< 10^{-4}$, permutation test), indicating ChromGene annotations are broadly informative of expression across cell types.

We also quantified how predictive ChromGene annotations are of gene expression and compared it to several baselines. To do this, we first separated genes into two groups: 'expressed' genes with RPKM ≥ 1 and 'unexpressed' genes with RPKM < 1. We held out genes on one chromosome at a time as a test set and used genes on all other chromosomes as a training set. We calculated the median expression for each ChromGene annotation for genes in the training set and used this as a predictor for the expression of genes in the held-out chromosome, and found that the ChromGene annotation was a strong predictor of whether genes were expressed or unexpressed (across 56 cell types: mean AUROC = 0.893, standard deviation = 0.021). We also calculated the mean squared error (MSE) and correlations of the predicted $\log_{10}$(RPKM + 0.1) expression compared to the corresponding observed expression values across all cell types, and we found that predicted expression values were close to the true expression (across 56 cell types: mean MSE = 0.418, standard deviation = 0.050; Pearson r = 0.763). We repeated the evaluations for the following three baselines (**Supp. Methods**):

<u>TSS Model</u>: Clusters genes based only on histone mark information at the TSS. This model only takes advantage of one position, and thus does not capture additional information throughout the gene.

<u>Gene Average Model</u>: Clusters genes based on the average histone mark values throughout the gene, which is equivalent to using ChromGene with only one state per HMM. This model has two key disadvantages: First, it does not take advantage of spatial information; instead, it treats heterogeneous spatial data as homogeneous, eliminating potentially useful information. Second, it

is more likely to be biased by gene length because histone marks preferentially associate with specific genic regions that scale differently with gene length (see below).

Collapsed Model: Clusters genes using a single state per mixture, as in the gene average model, but here the single state is found by first training a normal multi-state ChromGene model, then "collapsing" each multi-state HMM into a single-state HMM by taking the weighted average of the states in that mixture. This is meant to show that the differences between ChromGene and a single-state model are likely due to incorporating spatial information of histone marks instead of different instantiations of the models.

We implemented each baseline method to have an identical number of clusters as our ChromGene model. ChromGene annotations were significantly more predictive of gene expression than the three baseline methods (baseline AUROC = 0.818, 0.889, and 0.888; Pearson r = 0.601, 0.757, and 0.753; MSE = 0.685, 0.429, and 0.438; $p < 10^{-4}$ for all comparisons, paired binomial test, for TSS, Gene Average, and Collapsed Models, respectively).

ChromGene reduces association of gene length with clusters

We next analyzed the relationship between the ChromGene annotations and the length of genes assigned to it (**Fig. 5**). We found that the length distribution of most annotations was concentrated between 10k and 100kb with a large overlap of their distributions, but there were a few exceptions. Notably, 'low' and 'trans_cons' had median gene lengths around 100kb, while 'quiescent' was mostly composed of genes of less than 10kb length. This 'quiescent' annotation was strongly enriched (9.2 fold) for olfactory genes, which have a median length of 1034bp and are expressed at low levels in most cell types (mean expression=0.04 RPKM, median expression=0).

Because gene length distributions varied across ChromGene annotations, we wanted to ensure that ChromGene provided substantial information beyond gene length. We thus evaluated the amount of information shared between ChromGene annotations and gene length compared to annotations from the three baselines. Specifically, for each model and each cell type, we calculated the mutual information of the gene annotation and the gene length. We expected that the baseline TSS Model would share the least information with gene length, as it only incorporates data from the TSS and not the whole gene, while among the models that incorporate data from the whole gene, ChromGene would share the least information. Indeed, we found that across cell types, the TSS model had the lowest mutual information, and ChromGene annotations had significantly lower mutual information (mean of 0.31) than the Gene Average and Collapsed Models (mean of 0.46 and 0.48, respectively, $p < 10^{-30}$, binomial test, **Supp. Fig. 4**). This indicates that of models that use information throughout the gene, ChromGene annotations are least likely to simply reflect gene length.

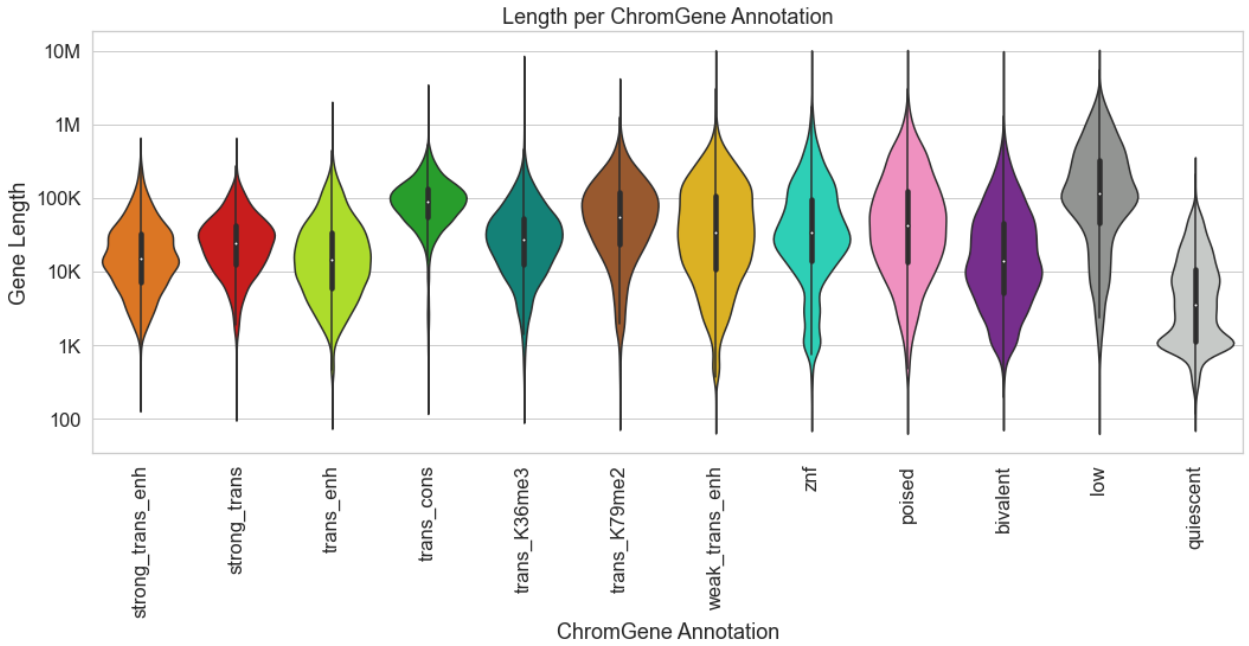

Figure 5: Lengths of genes by ChromGene annotation

Length distribution of different ChromGene annotations. Length axis is log-transformed for visualization.

ChromGene annotations capture cell type specific patterns

We next assessed how specific ChromGene assignments for the same gene vary across pairs of cell types. We first conducted enrichment analyses of ChromGene annotations across pairs of cell types relative to the number of genes assigned to each annotation (**Fig. 6**), excluding pairs of cell types that could be considered essentially biological replicates. As assignments of genes to different mixtures across cell types could be expected based on technical variability, we also estimated a confusion matrix for pairs of "replicate" cell types (**Supp. Fig. 5a**, **Methods**). We found 81.1% concordance in assignments between replicate cell types, as compared to 10.2% expected by the number of genes assigned to each mixture. We next followed a similar process to calculate a contingency table for non-replicates – the probability of a given gene being assigned to one mixture for one cell type given it was assigned to another mixture in another cell type (**Supp.**

Fig. 5b). We found that between pairs of randomly chosen non-replicate cell types, ChromGene annotations were 57.1% concordant, which is substantially lower than between replicates (81.1%) while substantially higher than random assignment (10.2%).

We further defined the "cell type specificity" of each ChromGene annotation by dividing the diagonal of the contingency table (across non-replicate cell types) by the confusion matrix diagonal (the probability biological replicates would be assigned to the same annotation), then subtracting this value from 1 to obtain a "cell type specificity score" so that higher values correspond to more cell-type specific annotations. We found that the annotations that varied the least across cell types were 'quiescent', 'strong_trans', 'znf', 'bivalent', and 'trans_K36me3' with cell type specificity scores from 0.16 to 0.24 (**Fig. 3**, **Supp. Table 1**). The most cell-type specific annotations were 'weak_trans_enh', 'low', and 'trans_enh' with scores of 0.49, 0.43, and 0.41 respectively. 'Weak_trans_enh' having the highest cell type specificity score is consistent with this annotation being primarily associated with enhancers (**Supp. Fig. 6**), which are known to be highly cell type specific [2, 29]. The 'low' annotation also had high cell type specificity despite having similarly low expression as the 'quiescent' annotation, and was often assigned to the mixtures 'poised' and 'bivalent' in other cell types.

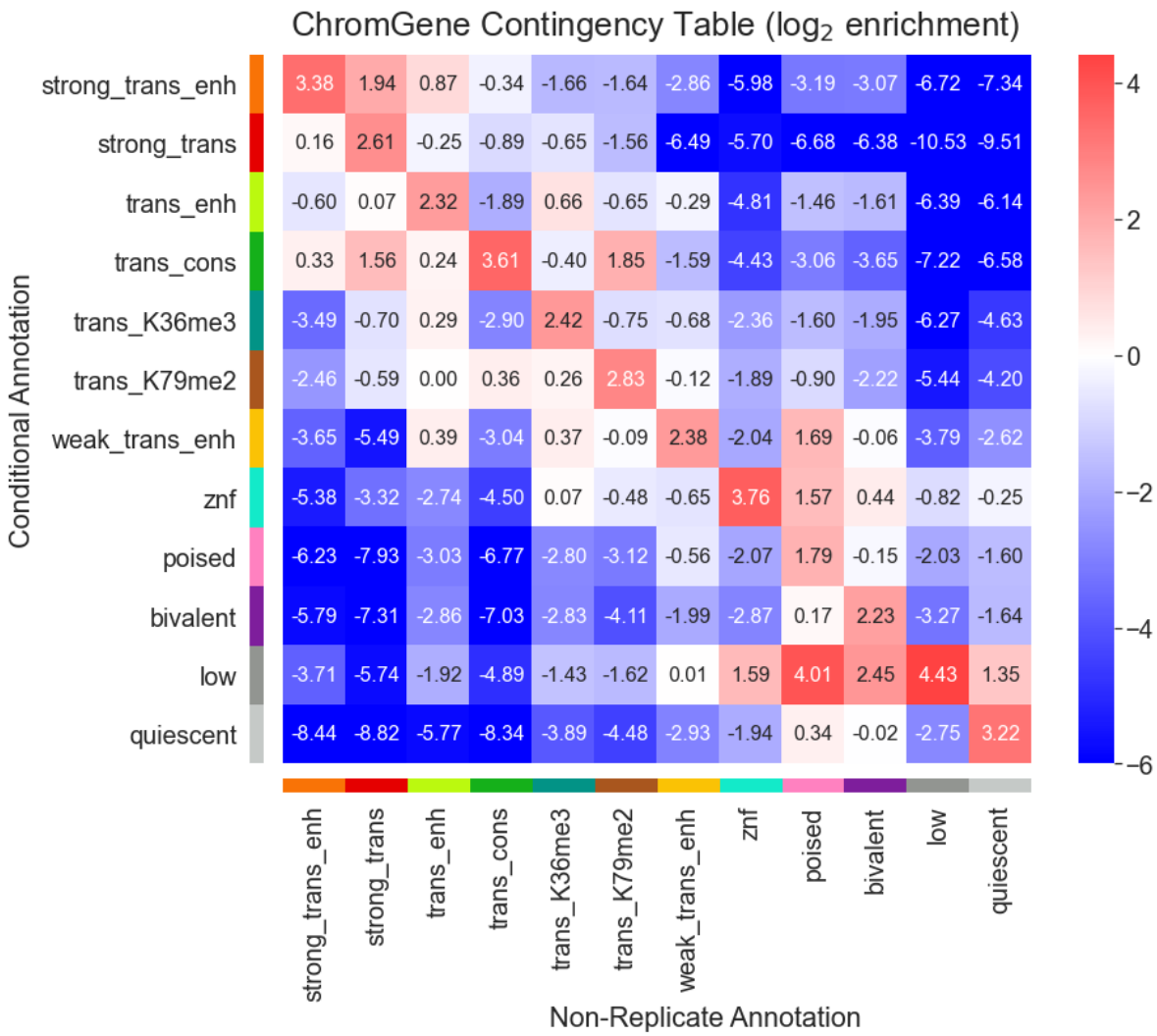

Figure 6: ChromGene contingency table enrichment

The $\log_2$ enrichment over all pairs of cell types for the combination of ChromGene assignments in the two cell types. Enrichment corresponds to an increased likelihood of two non-replicate cell types having the corresponding ChromGene assignments for a given gene, relative to randomly choosing based on ChromGene cluster sizes (**Methods**).

ChromGene mixtures are differentiated by gene set enrichments

We next analyzed the enrichment of ChromGene annotations with respect to various gene sets (**Supp. Table 1**). These gene sets included zinc finger named (ZNF) genes, constitutively

unexpressed genes, house-keeping genes, olfactory genes, 'biological processes' Gene Ontology (GO) terms, and cancer-related gene sets [1, 16, 30–34].

ZNF genes had the highest enrichment, 11.0 fold, for the 'znf' annotation (median $p < 10^{-200}$, hypergeometric test, **Methods**). Constitutively unexpressed genes (RPKM < 1 in all 56 cell types with matched expression available) [1] were most enriched (5.8 fold, $p < 10^{-300}$) in the 'quiescent' annotation. In contrast, a set of previously defined housekeeping genes, based on broad and constant expression levels [35], were most enriched (3.0 fold, $p < 10^{-300}$) for the 'strong_trans' annotation, which was 99% depleted for constitutively unexpressed genes. For olfactory genes [30], we observed the strongest enrichment in the 'quiescent' annotation (9.2 fold enrichment, $p < 10^{-200}$), which contained 75.1% of all olfactory genes.

For the GO term enrichments [31], we calculated an adjusted enrichment p-value for each GO term gene set for each cell type and ChromGene annotation (hypergeometric test, Bonferroni corrected for the number of combinations of 127 cell types, 12 ChromGene annotations and 6036 GO terms). For each ChromGene annotation, we identified GO terms that were enriched in the majority of cell types (adjusted $p < 0.01$) (**Methods**, **Supp. Fig. 7**, **Supp. Table 1**). The ChromGene annotations 'strong_trans_enh' and 'strong_trans' had the greatest number of such GO terms. The most significant terms for 'strong_trans_enh' and 'strong_trans' included core regulatory and metabolic processes with terms such as 'SRP-dependent cotranslational protein targeting to membrane' and cytoplasmic translation' for 'strong_trans_enh' and 'mRNA splicing, via spliceosome' and 'mRNA processing' for 'strong_trans'. The ChromGene annotation 'bivalent' had several neuron and development related enriched GO terms, including 'neuron differentiation' and 'anterior/posterior pattern specification'. In contrast the 'Quies' term, also associated with low expression, showed significant enrichments for terms such as 'sensory

perception of smell' consistent with its enrichment for olfactory genes. The different GO enrichments in some cases for mixtures with similar expression levels highlights the utility of ChromGene in extracting information beyond expression.

Across all 'biological process' GO terms, we found that the ChromGene annotations 'strong_trans_enh' and 'strong_trans', which had the highest expressed genes on average, were the most likely to be enriched, constituting 26% and 44% of the significant enrichments, respectively (**Supp. Fig. 8a**). Across all ChromGene annotations, we saw an average of 133 enriched GO terms per cell type (adjusted $p < 0.01$). This was substantially more than for the three baseline methods (TSS, Gene Average, Collapsed), where we saw an average of 53, 109, and 82 gene sets significantly enriched (adjusted $p < 0.01$), respectively. These results suggest that ChromGene annotations better correspond to existing biological knowledge as reflected in 'biological process' GO terms than the baseline methods.

For the cancer related gene sets, we used 967 gene sets produced by the Cancer Cell Line Encyclopedia implicated in various types of cancer [33] and, as before, performed a gene set enrichment analysis for each ChromGene annotation. Interestingly, we found that unlike for the 'biological process' GO terms, the significant enrichment for cancer gene sets were most likely to be found in lowly expressed annotations, particularly 'poised', 'bivalent', and 'low', which constituted the majority with 21%, 60%, and 16%, respectively (**Supp. Fig. 8b**). The enrichment of the poised and bivalent annotations is consistent with previous observations that misregulation of poised and bivalent chromatin regions are associated with cancer [36, 37]. In total, we found that ChromGene had an average of 151 cancer gene sets enriched per cell type. In comparison, the baseline methods (TSS, Gene Average, Collapsed) had 71, 72, and 70 gene sets enriched (hypergeometric test, $p < 0.01$, Bonferroni corrected for each combination of 127 cell types, 12

annotations, and 967 gene sets), respectively, substantially less than for ChromGene. These results further support that ChromGene annotations are more consistent with established biological gene sets than the baseline approaches.

ChromGene separates genes by pLI scores

We next explored the relationship between ChromGene annotations and genes with high pLI scores (≥ 0.9) [25]. Genes with high pLI scores have strong evidence that the gene is intolerant to loss of function, i.e., haploinsufficient.

The three ChromGene annotations most enriched for high pLI score genes were 'trans_cons', 'strong_trans_enh', and 'strong_trans' (**Fig. 7**). These annotations had an average of 46.8%, 36.1%, and 30.6% of its assigned genes, with high pLI scores across cell types, respectively, compared to 17.9% expected by chance. These three annotations were also among the top four most highly expressed annotations.

Notably, 'trans_cons' had a substantially larger percentage of high-pLI genes (46.8% and 13.0%, respectively) than 'trans_enh', despite a positive correlation between pLI score and expression (spearman r from 0.18 to 0.39, mean r=0.27 across cell types, all p-values < 10^{-100}, **Methods**), and 'trans_cons' having slightly lower overall expression than 'trans_enh' (median RPKM = 12.73 and 13.89, respectively). However, this difference is consistent with the substantial difference in gene length between the 'trans_cons' and 'trans_enh' annotations (**Fig. 5**), and a previously noted positive correlation between gene length and pLI [25]. Another difference between 'trans_cons' and 'trans_enh' is that genes annotated as 'trans_cons' are more likely than 'trans_enh' to be assigned to the 'strong_trans_enh' or 'strong_trans' annotations in other cell types (**Fig. 6**, **Supp. Fig. 5b**). Among the lowly expressed ChromGene annotations, 'low' and

'quiescent' had the greatest difference in average proportion of high pLI genes (16.3% and 0.8%, respectively). Compared to the 'quiescent' annotation, the 'low' annotation contained longer genes, and genes more likely to be assigned in other cell types to ChromGene annotations with a greater proportion of high pLI genes. Similar patterns also held when considering mean pLI (**Supp. Fig. 9**). These results further show that ChromGene captures additional information beyond expression.

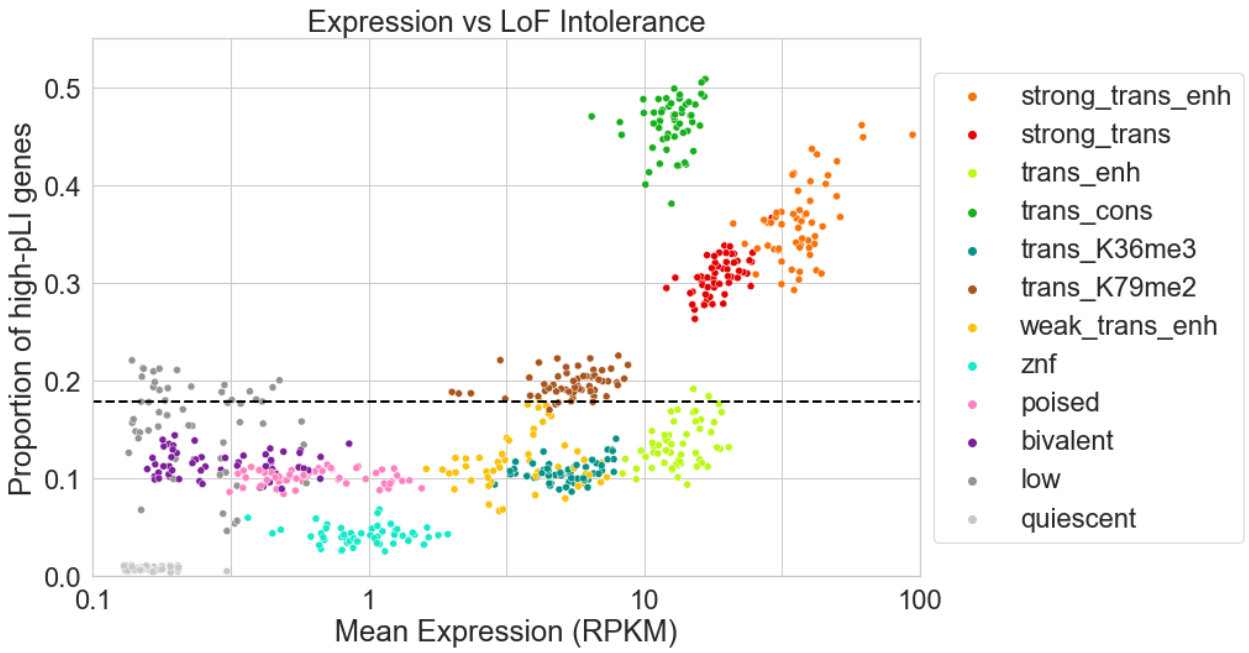

Figure 7: Expression and pLI scores per ChromGene annotation

Scatter plot showing on the axis x-the gene expression (RPKM) and on the y-axis the proportion of high pLI genes (pLI > 0.9). Each point corresponds to genes assigned to a specific ChromGene annotation in a single cell type. Points are colored by their ChromGene annotation. Dashed line corresponds to the overall proportion of genes with high pLI. The figure shows that although there is a positive association between the two measures, ChromGene captures information beyond expression. For example, 'trans_enh' and 'trans_cons' have similar expression levels, but substantially different proportions of high-pLI genes.

Discussion

Here, we introduced ChromGene, a principled, model-based method that uses a mixture of HMMs to annotate genes based on maps of multiple epigenetic marks across genes. ChromGene's focus on gene annotations is complementary to well established approaches for generating per-position annotations [9, 10].

We applied ChromGene to imputed data for 12 epigenomic marks to annotate genes in over 100 cell types. We showed that ChromGene annotations frequently reflect distinct gene expression levels. In cases where ChromGene annotations had similar gene expression levels, we found they differed on other important properties such as enrichment for high pLI score genes and gene set enrichments, reflecting that ChromGene annotations capture information beyond gene expression levels. We also showed that ChromGene yielded better agreement with gene expression data and more significant enrichments for cancer gene sets and GO terms than baseline approaches. We note that while ChromGene annotations will likely be preferable for many gene-centric analyses relative to per-position chromatin state annotations, it is likely less useful for when the object of study is not inherently gene centric, such as studying enrichments for GWAS identified variants.

There are multiple possible additional types of applications and extensions of ChromGene that can be investigated in future work. Although here, we applied ChromGene to protein-coding genes, ChromGene is more general and can also be applied to other pre-defined sets of genomic intervals such as long non-coding RNAs and pseudogenes. In this study, we combined our training data in a "concatenated" mode, where chromosomes across different cell types are treated as separate, and a single model is trained that applies to each epigenome. However, the input data for ChromGene can also be "stacked", where the emissions of marks across cell types are all observed simultaneously [26, 38]. This can be used to learn patterns of variation across cell types and

annotate genes based on them. In this study, we applied ChromGene on a set of 12-imputed data sets to define annotations based on a large number of cell types with a consistent set of input features. However, ChromGene can be applied with other choices for the input data.

We expect that the ChromGene annotations we have generated will be a useful resource for gene based analysis in and across many cell types, and that the approach will be useful for gene based annotations for data from additional marks, cell types, or species.

Methods

ChromGene model

For a single cell type, ChromGene uses a mixture of multivariate HMMs to model the combinatorial and spatial patterns within multiple epigenomic maps across a set of genes and to derive a single annotation per gene. Each gene is assumed to be generated by one of M fully-connected HMMs, each with S states. Each of these M HMMs is defined by three sets parameters: 1) initial probability for each state within each HMM, 2) the probability of transitioning from one state in the HMM to another state in the same HMM, and 3) the probability of observing each of E binarized emissions (in this case, histone marks or DNase mark) given a state in one of the HMMs. Although not explicitly trained, each HMM's prior probability of being chosen for a gene is equal to the sum of the initial probabilities of its states.

More formally, we denote mixtures as m, $1 \leq m \leq M$, where M is the total number of mixtures; S is the number of states per mixture, and each state s is $1 \leq s \leq S$. The total number of states is thus $M*S$, and each hidden state is denoted $h_{m,s}$, where m and s represent the mixture and state indices,

respectively. The initial probability, transition probabilities, and emission probabilities are defined follows:

Initial probabilities

The initial probability for each state, denoted $\tau_{m,s}$, corresponds to the probability that a randomly chosen gene starts in state $h_{m,s}$. The sum of all the initial probabilities of states in a mixture m corresponds to the initial probability of a gene starting in mixture m: $\tau_m = \sum_{s=1}^{S} \tau_{m,s}$, and the prior probability of the gene being assigned to mixture m.

Transition probabilities

Each mixture is modeled as a fully-connected HMM. The transition parameters $\alpha_{ms,ms'}$ correspond to the probability from a state s within mixture m transitioning to a state s' within the same mixture m. Transitions from states within one mixture to states in another mixture are not allowed.

Emission probabilities

The probability of observing a specific combination of marks in a state s of mixture m is determined based on a product of independent Bernoulli random variables over all marks in the state following the approach of ChromHMM [9]. The emissions parameters, $\beta_{m,s,e}$, correspond to the parameters of these Bernoulli random variables. $\beta_{m,s,e}$ and $(1 - \beta_{m,s,e})$ represent the probability of observing mark e as present or not present at a specific position in state $h_{m,s}$, respectively.

To apply ChromGene to multiple cell types, we apply the same modeling approach but treat data from multiple additional cell types as if they were additional genes in one cell type. This leads to a common model across cell types, but with cell type specific gene assignments. This approach is analogous to the 'concatenated' model learning approach of ChromHMM [2, 26].

Model Learning

Parameter initialization

The initial parameters of all mixture states are initialized to sum to 1 using a Dirichlet distribution with $\alpha_{m,s} = 1$. The emission parameters are initialized for each state by first randomly assigning each gene to one of the *M* mixtures. Then, each position in the genic region and flanks is assigned uniformly at random to one of the S states within that mixture. Finally, for each of the $M \times S$ hidden states, we set the initial emission probability of each epigenomic mark to its average frequency of being observed present across all positions assigned to the state. For each mixture *m* and each state *s* in the mixture, the transition parameters out of the state to each state in its mixture are initialized to sum to 1 using a Dirichlet distribution with $\alpha_s = 1$.

Expectation-Maximization procedure

After initializing parameters, ChromGene trains the parameters iteratively with the Baum-Welch algorithm, a special case of the Expectation-Maximization (EM) algorithm, until convergence. In the E step, ChromGene takes the current parameter values (emission, transition, and initial probabilities) and calculates the log likelihood of the data being observed given those values, $log(L(\theta; X, H)) = log(p(X, H|\theta))$, where $\theta = \{\theta_\tau, \theta_\alpha, \theta_\beta\}$, the set of initial, transition, and

emission parameters, respectively, X is the observed data, and H is the set of true, but hidden state assignments. In this step, we calculate the posterior probability of each position of each gene being generated by each of the $M \times S$ hidden states.

In the M step, these posterior probabilities are used to re-estimate the parameters θ so that the new parameter values maximize the expected likelihood in the E step, i.e., $\theta^{t+1} = \text{argmax}_{\theta} E[_{H|X,\theta^t} log(L(\theta; X, H))]$. In our application, we trained for 200 iterations, as is default in ChromHMM and parallelized the E-step computation across 8 cores. For faster computation, we also only evaluated on a different randomly selected subset of the data in each iteration (**Supp. Methods**).

Implementation

In our implementation, we generated special input files and trained the model on top of ChromHMM [9] (**Supp. Methods**). We trained models for M ranging from 8 to 20, and S ranging from 2 to 5. To balance model interpretability while capturing major biological distinctions, we chose the model with $M=12$ mixtures and $S=3$ states per mixture for all presented results.

Assignment of genes to mixtures

After training, ChromGene assigns each position along a gene a posterior probability of being in each of the hidden states $p(H_{m,s}|X)$. From this, ChromGene calculated the posterior probability of a gene being generated by each mixture: $P(m|X) = \sum_{s=1}^{S} p(H_{m,s}|X)$ based on any position. We note that all positions within a gene have the same mixture posterior probabilities; for example, if the first position of a gene has a posterior probability of 0.4 of being generated by mixture 1, then all positions within the gene have a posterior probability of 0.4 for mixture 1. This is a consequence

of transitions between mixtures being disallowed. We assigned each gene to the mixture $1 \leq m^* \leq M$ with the highest total posterior probability of generating the gene, i.e., $m^* = \text{argmax}_{m \in M} P(m|X)$. We used these hard assignments of genes to mixtures for all presented results.

Training data

To generate input data for ChromGene, we first defined our genes of interest. For this application, we used 19,919 protein coding genes as defined by Ensembl v65 / GENCODE v10 for hg19, as the epigenomic data we used had matching gene level expression estimates across 56 cell types based on these gene annotations [1, 16]. For each gene, we took its 5'-most base of the first exon and 3'-most base of the last exon as the TSS and TES of the gene, respectively. Genes on the negative strand were reversed to align with genes on the positive strand so all genes had the same orientation in the model. We rounded the TSS upstream (in the 3' direction) and the TES downstream (in the 5' direction) to the next position divisible by 200bp. We added an additional overhang of 2kb upstream of the first exon and downstream of the last exon to capture additional spatial information around the TSS and TES. We then binned the entire region (gene and overhangs) into 200bp bins so that the boundaries of each bin were divisible by 200. We then extracted the epigenomic marks, as described next.

To generate a single ChromGene model that would be comparable across a large number of cell types and marks, we used imputed data for a set of 12 marks (H3K36me3, H3K4me1, H3K4me2, H3K4me3, H3K9me3, H3K27ac, H3K27me3, H3K9ac, H3K79me2, H4K20me1, H2A.Z, and DNase) across 127 reference epigenomes, which for our purposes we treated and referred to as different cell types, except for calculation of the confusion matrix and contingency table, as

described below [1, 27]. This imputed data was previously used to train a 25-state ChromHMM model. The use of imputed data allowed us to annotate more cell types with the same set of marks compared to using directly observed data. We used the same binarization for the imputed data as previously generated [27] [Data available at https://egg2.wustl.edu/roadmap/data/byFileType/chromhmmSegmentations/binaryChmmInput/imputed12marks/binaryData/].

Gene expression data

We downloaded gene expression data for 56 cell types from the Roadmap Epigenomics Consortium [1] [available at https://egg2.wustl.edu/roadmap/data/byDataType/rna/expression/57epigenomes.RPKM.pc.gz]. We took the provided RPKM values, added a pseudocount of 0.1, and took the $\log_{10}$ transform of the value.

Gene expression analysis

To determine whether median gene expression variance within annotations was significantly smaller than across annotations, we performed a permutation test. Each median $\log_{10}$(RPKM+0.1) expression value for a cell type was randomly assigned to one of the ChromGene clusters, while maintaining 56 cell types per ChromGene cluster. We then calculated the mean within-ChromGene annotation variance of the median expression values for each permutation and for the true ChromGene annotation. To compute a p-value, we counted the fraction of 10,000 permutations in which the mean variance value based on the permuted values was less than that of the true ChromGene annotations.

Calculation of mutual information of assignment given gene length

To calculate mutual information of gene assignments given gene lengths, for each gene, we first calculated its $\log_{10}(length)$, which ranged from 2.06 to 6.73, where *length* is in bp. We binned the $\log_{10}(length)$ into 0.05-increment intervals to create a discretized distribution. Then, for each cell type, we calculated the mutual information of ChromGene assignment and the length bins, and repeated for the gene assignments based on each baseline method.

Calculation of confusion matrix

To generate a confusion matrix (**Supp. Fig. 5a**), we took our matrix of ChromGene assignments with entries $m_{g,c}$, where each of $g=1,...,19919$ corresponds to a gene and each of $c=1,...,127$ corresponds to a cell type (**Fig. 2**, genes subsampled and ordered for visualization). For each gene g, we calculated the conditional probability $P(m_{g,c} \mid m_{g,c'})$, where $c \neq c'$ correspond to pairs of epigenomes that were originally annotated as the same cell type but of different individuals ("Rectal Mucosa Donor 29" and "Rectal Mucosa Donor 31", "Foreskin Fibroblast Primary Cells skin01" and "Foreskin Fibroblast Primary Cells skin02", "Foreskin Melanocyte Primary Cells skin01" and "Foreskin Melanocyte Primary Cells skin03", "Foreskin Keratinocyte Primary Cells skin02" and "Foreskin Keratinocyte Primary Cells skin03", "Skeletal Muscle Female" and "Skeletal Muscle Male", "Primary hematopoietic stem cells G-CSF-mobilized Male" and "Primary hematopoietic stem cells G-CSF-mobilized Female", "Fetal Brain Female" and "Fetal Brain Male"). In short, we sought to answer the question: "*given an entry in the assignment matrix is* ***mixture i****, what is the probability that the same gene is assigned to* ***mixture j*** *in a replicate cell type?"* We then calculated overall conditional probabilities by averaging over all genes g. We

represented these conditional probabilities so that the mixture conditioned on corresponds to a row, which implies that each row sums to 1.

Calculation of gene contingency table

To generate the gene contingency table (**Supp. Fig. 5b**), we performed the same process as for the confusion matrix, but instead of calculating probabilities for pairs of "replicate" cell types, we calculated them for non-replicate cell types.

Cell type specificity

We defined the "cell type specificity" of each ChromGene annotation by dividing the diagonal of the contingency table (across non-replicate cell types) by the confusion matrix diagonal, then subtracting this value from 1 to obtain a "cell type specificity score" so that higher values correspond to more cell-type specific annotations.

Calculation of contingency table enrichment

To generate the contingency table enrichment (**Fig. 6**), we first generated an expected contingency table, where we assumed independence between assignments. For each ChromGene annotation, *m*, we calculated an empirical prior probability of observing the annotation assignment for a random cell type and gene $\pi_m = P(m) = \sum_{c=1}^{127} \sum_{g=1}^{19919} I(m_{g,c} = m) / (127 \times 19919)$, where $I(m_{g,c} = m)$ denotes the indicator function applied to the ChromGene assignment for gene g in cell type *c* being *m*. We took these prior probabilities and calculated an expected contingency table, where each entry *(i, j)* was found by multiplying the prior probabilities of mixtures m_i and m_j: $P(m_i) \times P(m_j)$. To calculate enrichments, we divided the observed contingency table (**Supp. Fig.**

5b) by the expected contingency table. Finally, we took the $\log_2$ of these values to show enrichments and depletions.

Olfactory and housekeeping gene annotations

We downloaded olfactory [30] and housekeeping gene annotations [35]. We matched the gene names to the GENCODE annotation [16] to label each gene as olfactory or not olfactory, and housekeeping or not housekeeping.

Gene set enrichments

To calculate the fold enrichments for ZNF named genes, housekeeping genes, constitutively unexpressed genes, and olfactory genes, for a mixture, we divided the mean proportion of genes from the set assigned to the mixture across all cell types by the mean proportion of all genes assigned to the mixture across all cell types. To calculate a median p-value for a gene set and mixture across cell types, we took each cell type and calculated a p-value using a hypergeometric test (scipy.stats.hypergeom, with X=[number of genes in mixture and gene set], M=[total number of genes], n=[total number of genes in gene set], N=[number of genes in mixture]), and then took the median of those values.

To calculate significant gene set enrichments for 'biological process' GO terms [31], we first found the overlap of a gene set with each of the ChromGene annotations (or baseline method) for a given cell type. Next, we calculated p-values using a hypergeometric test, as for the individual gene sets above, and corrected for multiple testing with a Bonferroni correction that controls for the number of combinations of cell types, mixtures, and GO terms tested. We repeated the process for each

baseline method. We then followed the same procedure for cancer gene sets [33]. The gene sets for 'biological process' GO terms and cancer gene sets were downloaded from the Enrichr database [34].

To generate the GO term enrichment median p-value heatmap (**Supp. Fig. 7**), we followed the same procedure. We removed rows where the median adjusted p-value was greater than our significance threshold of 0.01, and clustered rows using 'seaborn.clustermap', which uses a Euclidean metric and 'average' linking. Finally, we $-\log_{10}$ transformed the p-values for visualization.

ChromHMM state enrichment

For each ChromGene mixture, we took all genes and cell types assigned to the mixture, and counted the total observed counts of each ChromHMM state in a previously described 25-state model [27], thus yielding a matrix of *M* ChromGene mixtures by 25 ChromHMM states. We then added a pseudocount of 1 to these counts and normalized the rows (ChromGene mixtures) to unit probability. We divided these probabilities by the genome-wide ChromHMM state assignment proportions across all cell types to generate an enrichment, and finally, calculated the $\log_2$ of these enrichments (**Supp. Fig. 6**).

pLI score analysis

For pLI score analysis, we obtained pLI scores for each gene from gnomAD [25] [https://storage.googleapis.com/gnomad-public/release/2.1.1/constraint/gnomad.v2.1.1.lof_metrics.by_gene.txt.bgz, "exac_pLI" column] .

For correlating gene pLI scores with gene expression, for each of the 56 cell types with expression data available [1], we correlated the expression value of genes with their corresponding pLI scores using spearman correlation.

Declarations

Ethics approval and consent to participate

Not applicable

Consent for Publication

Not applicable

Availability of Data and Materials

The ChromGene annotations generated in this study and the ChromGene software are available in the ErnstLab ChromGene GitHub repository, https://github.com/ernstlab/ChromGene. ChromGene annotations are also available as a Supplementary Data file.

Competing Interests

The authors declare no competing interests.

Funding

This work was supported by the U.S. National Institutes of Health [grants T32HG002536 (A.J.), R01ES024995, U01HG007912, DP1DA044371, UH3NS104095, U01HG012079 (J.E.)], the National Science Foundation [1254200, 2125664] (J.E.), an Alfred P. Sloan Fellowship (J.E.), Rose Hills Innovator

Award, and the UCLA Jonsson Comprehensive Cancer Center and Eli and Edythe Broad Center of Regenerative Medicine and Stem Cell Research Ablon Scholars Program.

Authors' Contributions

AJ and JE developed the method. AJ implemented the method and performed all analyses presented. AJ and JE wrote the manuscript. Both authors read and approved the final manuscript.

Acknowledgements

We thank Huiling Huang for conducting some preliminary analyses of the results of the method. We also thank Adriana Arneson and Petko Fiziev, and other past and current members of the Ernst Lab, for their feedback on this work.

References

1. Kundaje A, Meuleman W, Ernst J, Bilenky M, Yen A, Heravi-Moussavi A, et al. Integrative analysis of 111 reference human epigenomes. Nature. 2015;518:317–30.

2. Ernst J, Kheradpour P, Mikkelsen TS, Shoresh N, Ward LD, Epstein CB, et al. Mapping and analysis of chromatin state dynamics in nine human cell types. Nature. 2011;473:43–9.

3. Barski A, Cuddapah S, Cui K, Roh T-Y, Schones DE, Wang Z, et al. High-Resolution Profiling of Histone Methylations in the Human Genome. Cell. 2007;129:823–37.

4. ENCODE Project Consortium. An integrated encyclopedia of DNA elements in the human genome. Nature. 2012;489:57–74.

5. Boyle AP, Song L, Lee B-K, London D, Keefe D, Birney E, et al. High-resolution genome-wide in vivo footprinting of diverse transcription factors in human cells. Genome Res. 2011;21:456–64.

6. Buenrostro JD, Giresi PG, Zaba LC, Chang HY, Greenleaf WJ. Transposition of native chromatin for fast and sensitive epigenomic profiling of open chromatin, DNA-binding proteins and nucleosome position. Nat Methods. 2013;10:1213–8.

7. Stunnenberg HG, International Human Epigenome Consortium, Hirst M. The International Human Epigenome Consortium: A Blueprint for Scientific Collaboration and Discovery. Cell. 2016;167:1145–9.

8. Ernst J, Kellis M. Discovery and characterization of chromatin states for systematic annotation of the human genome. Nat Biotechnol. 2010;28:817–25.

9. Ernst J, Kellis M. ChromHMM: automating chromatin state discovery and characterization. Nat Methods. 2012;9:215–6.

10. Hoffman MM, Buske OJ, Wang J, Weng Z, Bilmes JA, Noble WS. Unsupervised pattern discovery in human chromatin structure through genomic segmentation. Nat Methods. 2012;9:473–6.

11. Claussnitzer M, Dankel SN, Kim K-H, Quon G, Meuleman W, Haugen C, et al. FTO Obesity Variant Circuitry and Adipocyte Browning in Humans. N Engl J Med. 2015;373:895–907.

12. Libbrecht MW, Chan RCW, Hoffman MM. Segmentation and genome annotation algorithms for identifying chromatin state and other genomic patterns. PLOS Comput Biol. 2021;17:e1009423.

13. Wang Z, Gerstein M, Snyder M. RNA-Seq: a revolutionary tool for transcriptomics. Nat Rev Genet. 2009;10:57–63.

14. Mortazavi A, Williams BA, McCue K, Schaeffer L, Wold B. Mapping and quantifying mammalian transcriptomes by RNA-Seq. Nat Methods. 2008;5:621–8.

15. Eisen MB, Spellman PT, Brown PO, Botstein D. Cluster analysis and display of genome-wide expression patterns. Proc Natl Acad Sci. 1998;95:14863–8.

16. Frankish A, Diekhans M, Ferreira A-M, Johnson R, Jungreis I, Loveland J, et al. GENCODE reference annotation for the human and mouse genomes. Nucleic Acids Res. 2019;47:D766–73.

17. Su D, Wang X, Campbell MR, Song L, Safi A, Crawford GE, et al. Interactions of Chromatin Context, Binding Site Sequence Content, and Sequence Evolution in Stress-Induced p53 Occupancy and Transactivation. PLOS Genet. 2015;11:e1004885.

18. Zhu W, Hu B, Becker C, Doğan ES, Berendzen KW, Weigel D, et al. Altered chromatin compaction and histone methylation drive non-additive gene expression in an interspecific Arabidopsis hybrid. Genome Biol. 2017;18:157.

19. Kharchenko PV, Alekseyenko AA, Schwartz YB, Minoda A, Riddle NC, Ernst J, et al. Comprehensive analysis of the chromatin landscape in Drosophila melanogaster. Nature. 2011;471:480–5.

20. Sahu A, Li N, Dunkel I, Chung H-R. EPIGENE: genome-wide transcription unit annotation using a multivariate probabilistic model of histone modifications. Epigenetics Chromatin. 2020;13:20.

21. Marco E, Meuleman W, Huang J, Glass K, Pinello L, Wang J, et al. Multi-scale chromatin state annotation using a hierarchical hidden Markov model. Nat Commun. 2017;8:15011.

22. Jaschek R, Tanay A. Spatial Clustering of Multivariate Genomic and Epigenomic Information. 2009. p. 170–83.

23. Larson JL, Huttenhower C, Quackenbush J, Yuan G-C. A tiered hidden Markov model characterizes multi-scale chromatin states. Genomics. 2013;102:1–7.

24. Ge X, Zhang H, Xie L, Li WV, Kwon SB, Li JJ. EpiAlign: an alignment-based bioinformatic tool for comparing chromatin state sequences. Nucleic Acids Res. 2019;47:e77.

25. Lek M, Karczewski KJ, Minikel EV, Samocha KE, Banks E, Fennell T, et al. Analysis of protein-coding genetic variation in 60,706 humans. Nature. 2016;536:285–91.

26. Ernst J, Kellis M. Chromatin-state discovery and genome annotation with ChromHMM. Nat Protoc. 2017;12:2478–92.

27. Ernst J, Kellis M. Large-scale imputation of epigenomic datasets for systematic annotation of diverse human tissues. Nat Biotechnol. 2015;33:364–76.

28. Heintzman ND, Stuart RK, Hon G, Fu Y, Ching CW, Hawkins RD, et al. Distinct and predictive chromatin signatures of transcriptional promoters and enhancers in the human genome. Nat Genet. 2007;39:311–8.

29. Heintzman ND, Hon GC, Hawkins RD, Kheradpour P, Stark A, Harp LF, et al. Histone modifications at human enhancers reflect global cell-type-specific gene expression. Nature. 2009;459:108–12.

30. Barnes IHA, Ibarra-Soria X, Fitzgerald S, Gonzalez JM, Davidson C, Hardy MP, et al. Expert curation of the human and mouse olfactory receptor gene repertoires identifies conserved coding regions split across two exons. BMC Genomics. 2020;21:196.

31. Ashburner M, Ball CA, Blake JA, Botstein D, Butler H, Cherry JM, et al. Gene Ontology: tool for the unification of biology. Nat Genet. 2000;25:25–9.

32. Kuleshov MV, Jones MR, Rouillard AD, Fernandez NF, Duan Q, Wang Z, et al. Enrichr: a comprehensive gene set enrichment analysis web server 2016 update. Nucleic Acids Res. 2016;44:W90-97.

33. Barretina J, Caponigro G, Stransky N, Venkatesan K, Margolin AA, Kim S, et al. The Cancer Cell Line Encyclopedia enables predictive modelling of anticancer drug sensitivity. Nature. 2012;483:603–7.

34. Chen EY, Tan CM, Kou Y, Duan Q, Wang Z, Meirelles GV, et al. Enrichr: interactive and collaborative HTML5 gene list enrichment analysis tool. BMC Bioinformatics. 2013;14:128.

35. Eisenberg E, Levanon EY. Human housekeeping genes, revisited. Trends Genet TIG. 2013;29:569–74.

36. Chaffer CL, Marjanovic ND, Lee T, Bell G, Kleer CG, Reinhardt F, et al. Poised chromatin at the ZEB1 promoter enables breast cancer cell plasticity and enhances tumorigenicity. Cell. 2013;154:61–74.

37. Bernhart SH, Kretzmer H, Holdt LM, Jühling F, Ammerpohl O, Bergmann AK, et al. Changes of bivalent chromatin coincide with increased expression of developmental genes in cancer. Sci Rep. 2016;6:37393.

38. Vu H, Ernst J. Universal annotation of the human genome through integration of over a thousand epigenomic datasets. Genome Biol. 2022;23:9.

Supplementary Methods

Implementation on top of ChromHMM

To implement ChromGene on top of ChromHMM, we first observed that a mixture of HMMs can be defined in terms of a single HMM with certain transitions disallowed. Specifically, given a set of *M* fully-connected HMMs, each acting as a mixture component, this can be represented with a single, larger HMM with the addition of a "dummy state" and "dummy mark." In the single HMM, each non-dummy state of the HMM can transition into and out of other states within its mixture and a single "dummy state", but not directly to states of other HMM mixtures (**Supp. Fig. 1a,b**). From the "dummy state", transitioning to any mixture is allowed, but only through the use of the "dummy mark", which forces transitions into and out of the "dummy state".

We structured the input data so that all genes in a chromosome and cell type (after adding 2kb overhangs and reversing genes on the negative strand) were concatenated head to tail, but with a single "dummy position" separating the genes, and a dummy position at the beginning and end of the data. In this dummy position, the emission for all the original input marks is set to 0, but we include an emission of 1 for a single, new mark designated the "dummy mark" (**Supp. Fig. 1c**). This dummy mark has an emission of 0 within all extended genic regions, and 1 only for the dummy position (**Supp. Fig. 1d**). Upon reaching the dummy position, the model is forced to transition to the dummy state. After this dummy state, the hidden state can transition to any of the mixture components.

This structure also allowed us to compactly represent all genes without having a separate file for each gene. For a single cell type, we had 23 chromosome files (chromosomes 1-22 and X). For 127 cell types, this yielded $127 \times 23 = 2921$ total input data files.

Similarly, we generated initial parameter files for the initial parameters described in the Methods section. For M mixture components, S states per mixture, and the dummy state, we had a total of $(M \times S) + 1$ states. The initial probability for each state in each mixture is set to 0, except for the dummy state, which is set to 1. The transition probabilities from any state in a mixture to each other state in the same mixture was allowed to be nonzero, and normalized so that the sum of these probabilities was 0.95. The remaining 0.05 probability was set to be the probability of transitioning from the mixture's states to the dummy state. The probability of transitions from the dummy state to each of the other $M \times S$ states corresponds to the initial parameters, which, as described (**Methods**), were initialized using a Dirichlet distribution with $\alpha_{m,s} = 1$ for all mixtures so that they summed to 1. The transition probability from a state in a mixture to each state in different mixtures was set to 0.

Finally, the emission probabilities were initialized as described in the Methods section, except that for the dummy state, the emission probability of the epigenomic marks was set to 0, and the emission of the dummy mark was set to 1; for remaining genomic states, the emission probabilities for the dummy mark was set to 0, and probabilities for the epigenomic marks were not restricted.

We passed the data and the initialized parameter files into ChromHMM's LearnModel function and used several optional flags. We used the -e 0 and -t 0 flags to enforce that a 0 or 1 emission or transition parameter in the initial parameter file remains at that value. We also used the -scalebeta flag to increase numerical stability. With the -scalebeta flag, ChromHMM rescales the backward variables based on the sum of their values at a position as opposed to reusing the scaling value for

the forward variables. We observed that this was necessary in some cases to prevent overflow in this setting. We used the flag -n 100 to sample 100 files for each iteration, and -d -1 to allow the log likelihood to increase between iterations. The log likelihood can increase between iterations because different subsamples of the data are evaluated on different iterations. We trained for 200 iterations, as default in ChromHMM, using ChromHMM v1.18.

After training the model, we used ChromHMM to generate posterior probability assignment files from which we calculated the posterior probabilities of each gene in each cell type being generated by each of the *M* HMMs and computed the maximum to derive hard assignments.

ChromGene annotation visualization

To visualize ChromGene annotations across cell types and genes, we first randomly subsampled the 19,919 protein-coding genes to 2000 genes. For the ChromGene annotations for these 2000 genes, we calculated a pairwise distance between them as $(1 - mean(I(X_i = Y_i))$, where X_i and Y_i corresponded to the ChromGene assignments across the 127 cell types and $I(x)$ is the indicator function. Columns, which correspond to cell types, were ordered the same way as previously [1]. Rows were ordered using scipy's hierarchical clustering function, using optimal leaf ordering and average (UPGMA) linkage.

Baseline model implementations

TSS model

To generate a 12-state model based only on gene TSSs, we took histone mark binarization data across the 127 cell types for the 19,919 genes, and used the data at the TSS position, rounded down

to the closest 200bp bin. As with the standard ChromGene input data, we separated these individual TSS positions by a single dummy position, then trained a 12-state model on top of ChromHMM, and followed the same procedures for generating annotations.

Gene average model

The gene average model was implemented using ChromGene, but used a single hidden state per mixture (i.e., M=12 mixtures, S=1 states per mixture). All other procedures were identical.

Collapsed model

The collapsed model was identical in structure to the gene average model (M=12 mixtures, S=1 states per mixture), but was not trained directly. After training the full ChromGene model (M=12 mixtures, S=3 states per mixture), as is used in all results presented, we calculated the prior probability of a collapsed mixture by summing the initial probabilities within its corresponding mixture of the full model. If the initial probabilities for the S states within a mixture m are denoted $\tau_{m,s}$, then the initial probability for the collapsed state s' of the corresponding mixture m' is equal to the prior probability of mixture m: $\tau_{s'} = \pi_m = \sum_{s=1}^{S} \tau_{m,s}$. The transition probability from the dummy state to a mixture is this prior probability. The transition probabilities of the collapsed state to itself is calculated by comparing the number of observed state assignments for the corresponding mixture in the full model to the number of genes assigned to that mixture. If the number of 200bp positions assigned to some mixture is denoted x_m, and the number of genes assigned to that mixture is denoted n_m, then there are (x_m-n_m) transitions from the mixture to itself and n_m transitions from the mixture to the dummy state, for a total of x_m transitions. We set the transition probability of the

collapsed state to itself as $(x_m - n_m)/x_m$ and the transition probability of the collapsed state to the dummy state as n_m/x_m.

The emission probability parameters of the collapsed model are set to the weighted mean of the probabilities of the full model, weighted by the state prior probabilities. If the emission probability for state *s* in mixture *m* for mark *e* is denoted $\beta_{m,s,e}$, the emission probability of the corresponding collapsed mixture *m'* with the single collapsed state s' is $\beta_{m',s',e} = \sum_{s=1}^{S} \pi_{m,s}\beta_{m,s,e}$, where $\pi_{m,s}$ is the prior probability of state *s* in mixture *m*, and is equal to the fraction of 200bp bins assigned to state *s* across all cell types and genes. These parameters are all set in the ChromHMM model file, and are used directly without training to generate assignments for all genes and cell types.

Supplementary Figures

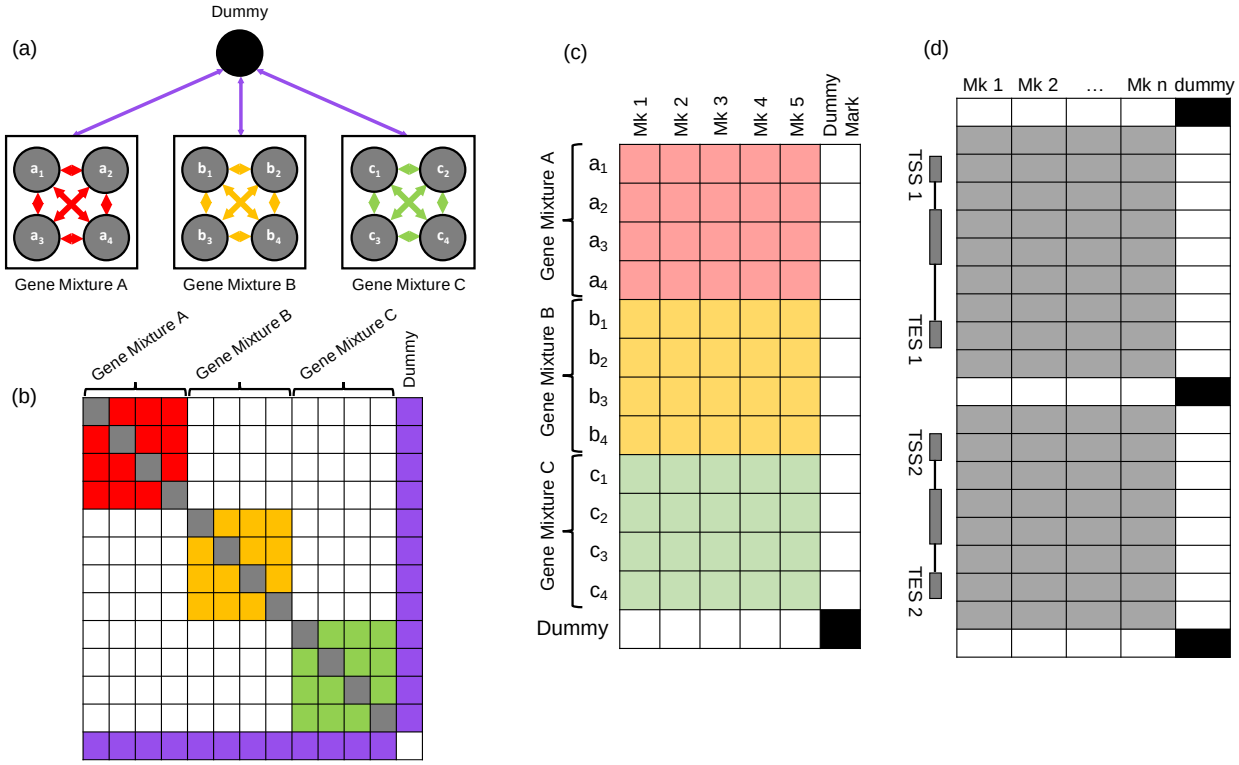

Supplementary Figure 1: Schematic of ChromGene implementation on top of ChromHMM

(a) Diagram showing *M*=3 ChromGene mixtures (*S*=4 states per mixture in each black box), connected by the "dummy state", which is used for implementation on top of ChromHMM.

(b) Transition matrix for example model. Transitions are allowed within each mixture (within red, within yellow, within green), but transitions are not allowed directly between mixtures. Transitions are allowed from any mixture to the dummy state, or from the dummy state to any mixtures, but transitions only occur at the single "dummy position" between genes.

(c) Example emission matrix. All states within mixtures A, B, and C (denoted $a_1 \ldots c_4$) have an emission probability between 0 and 1 (light red, yellow, and green) for the five marks, and an emission probability enforced to be 0 (white) for the "dummy mark" (last column). The "dummy state" (last row) has an

emission probability enforced to be 0 for all marks except for the "dummy mark", for which the emission probability is set to 1 (black).

(d) Example input data. At the dummy position, only the dummy mark is emitted (right column, black), and no other marks are emitted at that position (white). Within the gene body, epigenomic marks may be emitted (grey), but the dummy mark cannot (white). Only the dummy state can emit the dummy mark. This enforces that the dummy state is observed between genes to allow sequential genes to be assigned to different mixtures.

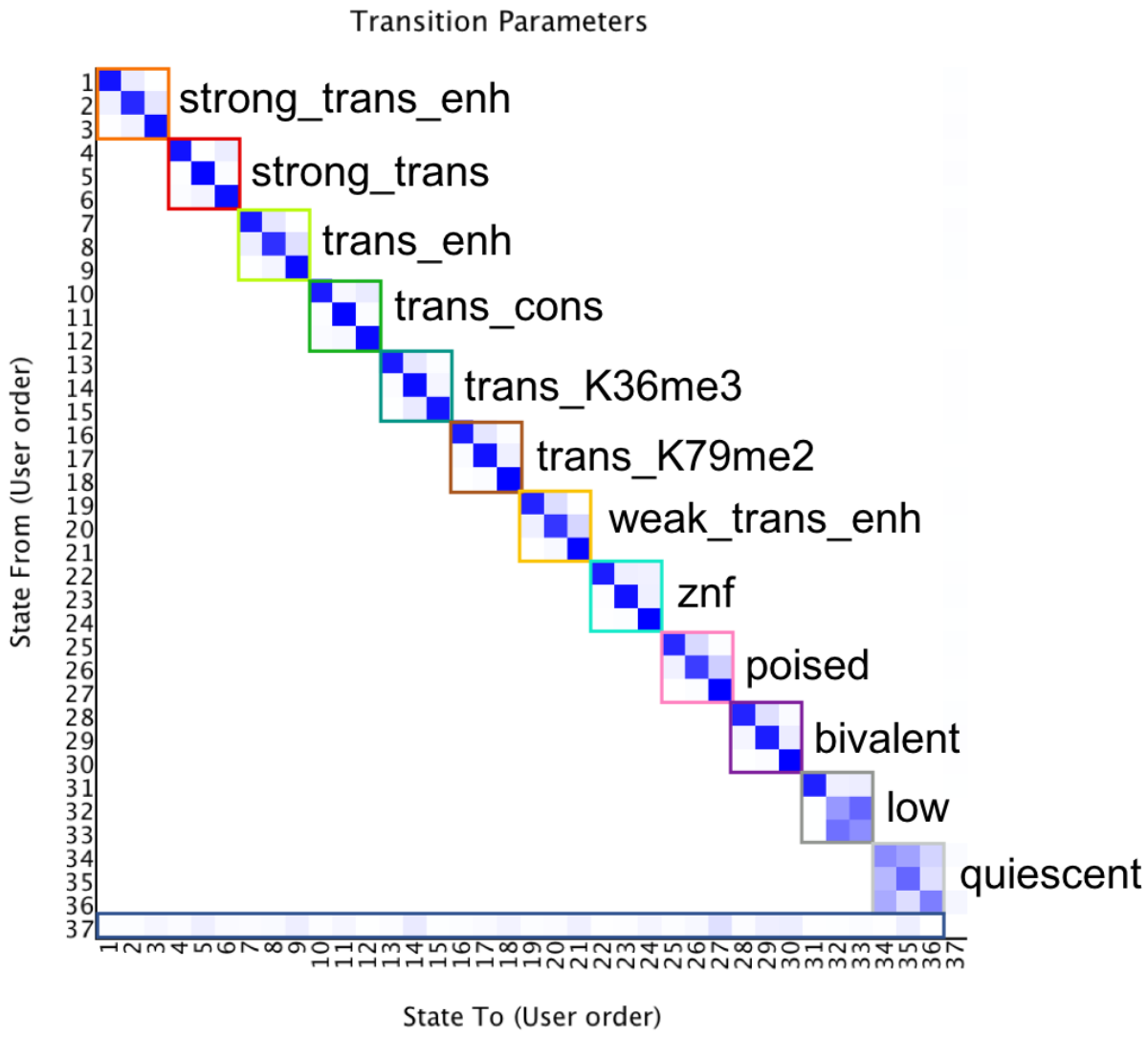

Supplementary Figure 2: ChromGene state transitions

Transition parameters between states within each mixture are marked in 3x3 squares. The bottom bar represents the initial probability of each state, independent of mixture. The mixture prior probabilities are the sums of the initial probabilities for their corresponding states. Transition probabilities are reported in (**Supp. Table 1**).

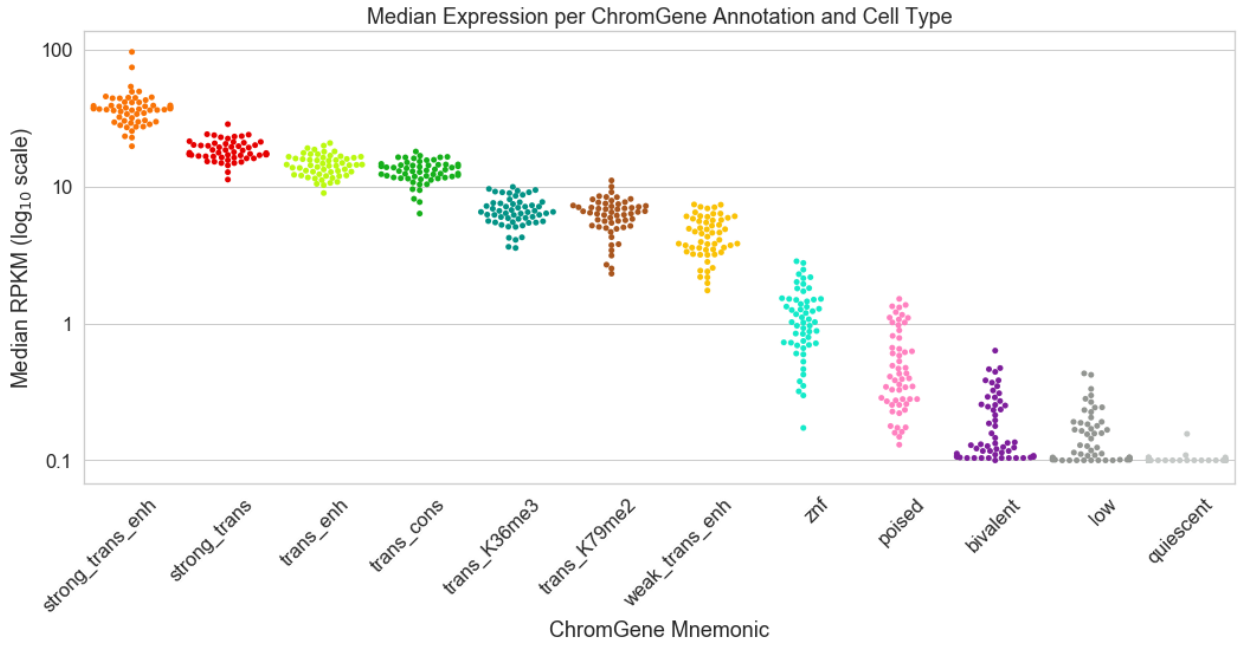

Supplementary Figure 3: Median Expression for each ChromGene assignment, separated by cell type

Distribution of median expression (RPKM) per ChromGene assignment. To generate this, for each of 56 cell types with expression data, and for ChromGene assignment, we took all genes assigned to the ChromGene assignment and calculated the median expression. Each point represents a single cell type and ChromGene assignment.

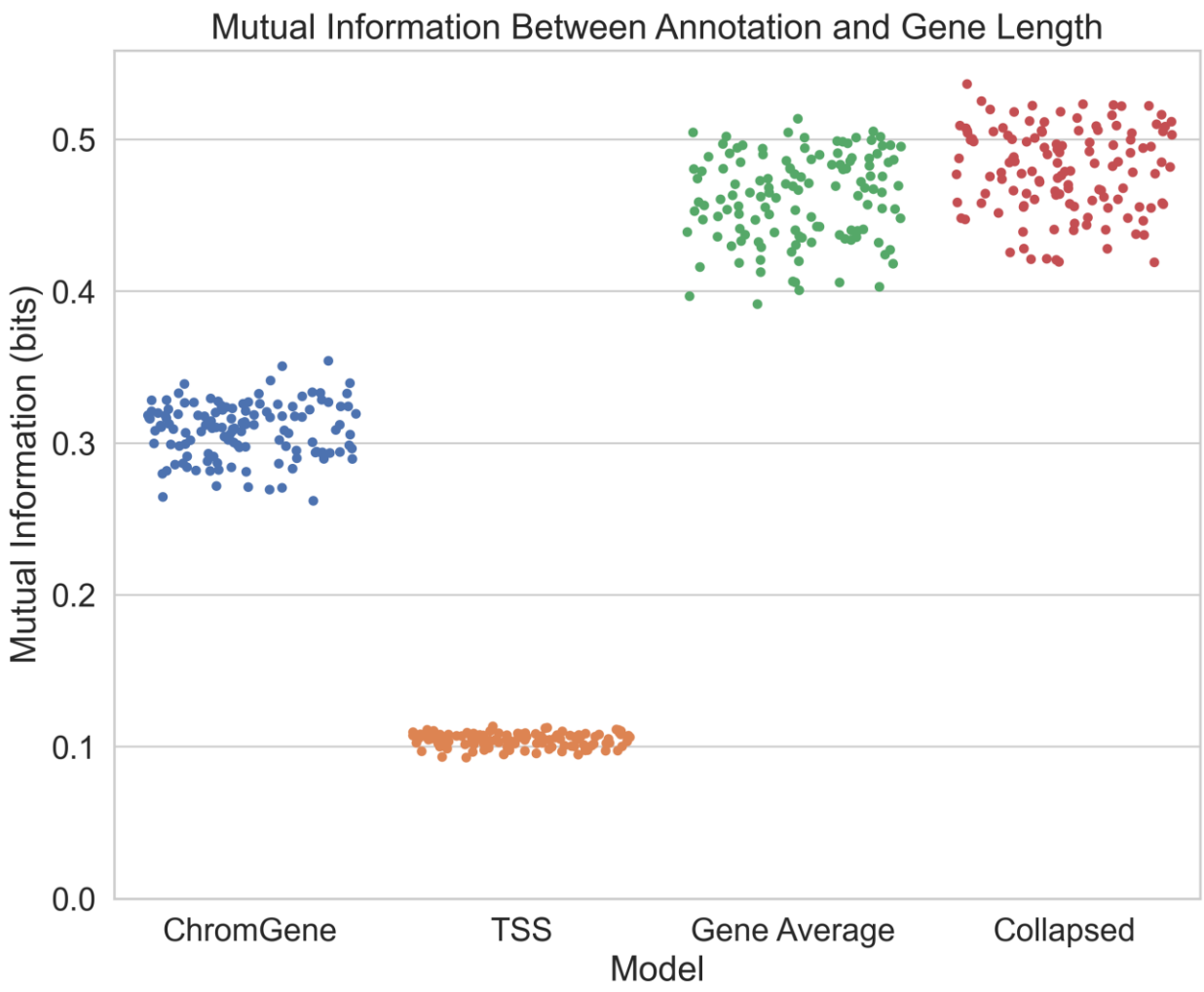

Supplementary Figure 4: Mutual information of annotation and gene length

The mutual information of annotations and gene lengths, where each point represents a cell type. Horizontal axis: ChromGene and three baselines: TSS, gene average, and collapsed models. ChromGene assignments have less information shared with the gene length ($p < 10^{-30}$, binomial test), indicating that ChromGene annotations are less likely to directly reflect information about gene length compared to baseline methods that incorporate information from the whole gene. Annotations from the TSS model have the lowest mutual information with gene length, as expected, given it only uses information at the TSS.

(a)

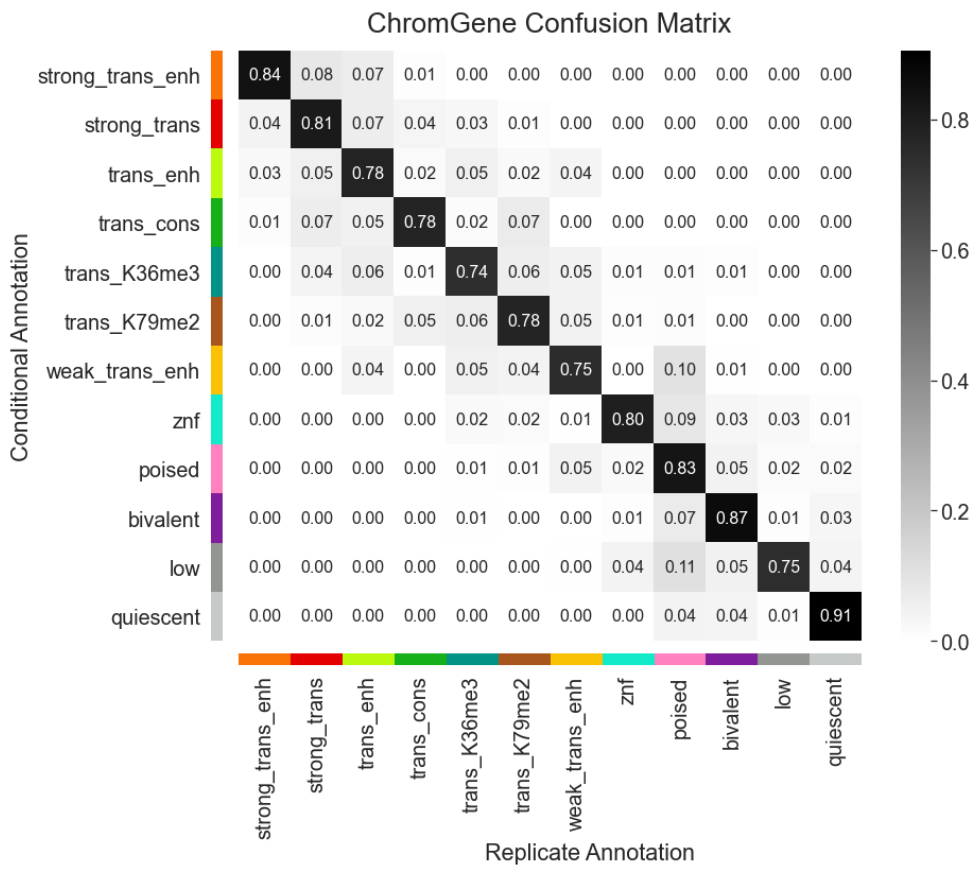
ChromGene Confusion Matrix
Conditional Annotation
strong_trans_enh 0.84 0.08 0.07 0.01 0.00 0.00 0.00 0.00 0.00 0.00 0.00 0.00
strong_trans 0.04 0.81 0.07 0.04 0.03 0.01 0.00 0.00 0.00 0.00 0.00 0.00
trans_enh 0.03 0.05 0.78 0.02 0.05 0.02 0.04 0.00 0.00 0.00 0.00 0.00
trans_cons 0.01 0.07 0.05 0.78 0.02 0.07 0.00 0.00 0.00 0.00 0.00 0.00
trans_K36me3 0.00 0.04 0.06 0.01 0.74 0.06 0.05 0.01 0.01 0.01 0.00 0.00
trans_K79me2 0.00 0.01 0.02 0.05 0.06 0.78 0.05 0.01 0.01 0.00 0.00 0.00
weak_trans_enh 0.00 0.00 0.04 0.00 0.05 0.04 0.75 0.00 0.10 0.01 0.00 0.00
znf 0.00 0.00 0.00 0.00 0.02 0.02 0.01 0.80 0.09 0.03 0.03 0.01
poised 0.00 0.00 0.00 0.00 0.01 0.01 0.05 0.02 0.83 0.05 0.02 0.02
bivalent 0.00 0.00 0.00 0.00 0.01 0.00 0.00 0.01 0.07 0.87 0.01 0.03
low 0.00 0.00 0.00 0.00 0.00 0.00 0.00 0.04 0.11 0.05 0.75 0.04
quiescent 0.00 0.00 0.00 0.00 0.00 0.00 0.00 0.00 0.04 0.04 0.01 0.91
0.8
0.6
0.4
0.2
0.0
strong_trans_enh
strong_trans
trans_enh
trans_cons
trans_K36me3
trans_K79me2
weak_trans_enh
znf
poised
bivalent
low
quiescent
Replicate Annotation

(b)

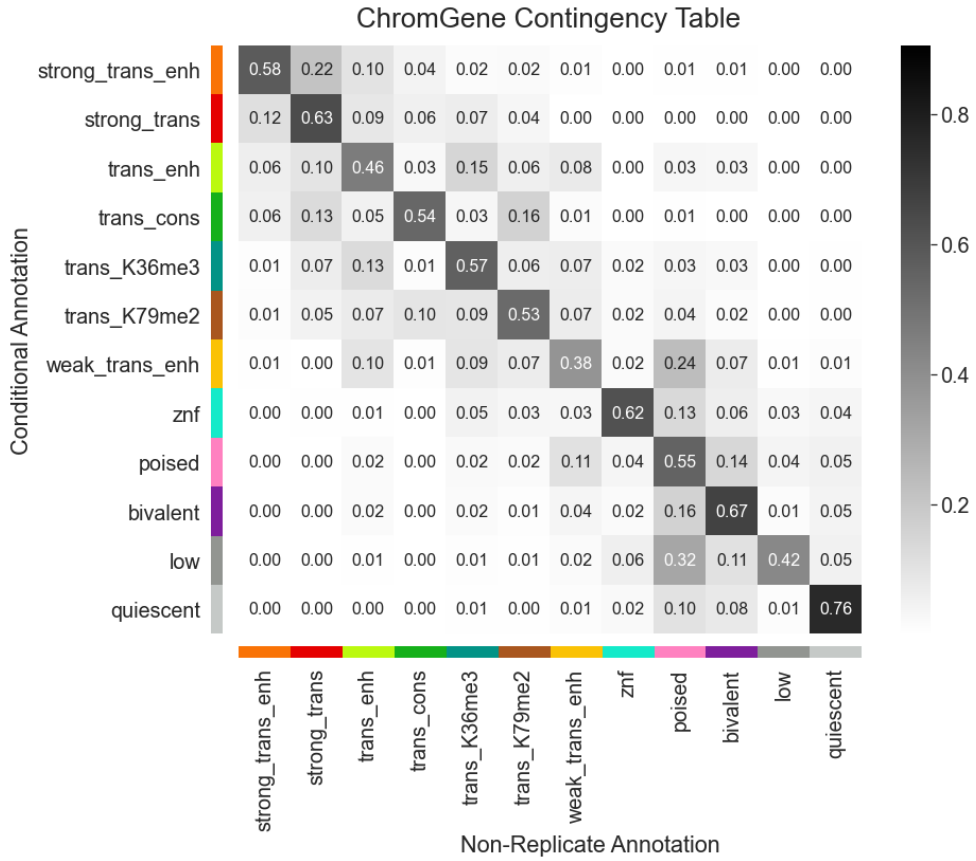
ChromGene Contingency Table
Conditional Annotation
strong_trans_enh 0.58 0.22 0.10 0.04 0.02 0.02 0.01 0.00 0.01 0.01 0.00 0.00
strong_trans 0.12 0.63 0.09 0.06 0.07 0.04 0.00 0.00 0.00 0.00 0.00 0.00
trans_enh 0.06 0.10 0.46 0.03 0.15 0.06 0.08 0.00 0.03 0.03 0.00 0.00
trans_cons 0.06 0.13 0.05 0.54 0.03 0.16 0.01 0.00 0.01 0.00 0.00 0.00
trans_K36me3 0.01 0.07 0.13 0.01 0.57 0.06 0.07 0.02 0.03 0.03 0.00 0.00
trans_K79me2 0.01 0.05 0.07 0.10 0.09 0.53 0.07 0.02 0.04 0.02 0.00 0.00
weak_trans_enh 0.01 0.00 0.10 0.01 0.09 0.07 0.38 0.02 0.24 0.07 0.01 0.01
znf 0.00 0.00 0.01 0.00 0.05 0.03 0.03 0.62 0.13 0.06 0.03 0.04
poised 0.00 0.00 0.02 0.00 0.02 0.02 0.11 0.04 0.55 0.14 0.04 0.05
bivalent 0.00 0.00 0.02 0.00 0.02 0.01 0.04 0.02 0.16 0.67 0.01 0.05
low 0.00 0.00 0.01 0.00 0.01 0.01 0.02 0.06 0.32 0.11 0.42 0.05
quiescent 0.00 0.00 0.00 0.00 0.01 0.00 0.01 0.02 0.10 0.08 0.01 0.76
0.8
0.6
0.4
0.2
strong_trans_enh
strong_trans
trans_enh
trans_cons
trans_K36me3
trans_K79me2
weak_trans_enh
znf
poised
bivalent
low
quiescent
Non-Replicate Annotation

906

Supplementary Figure 5: ChromGene confusion matrix and contingency table

(a) Confusion matrix for ChromGene annotations between pairs of cell types that can be treated as biological replicates. (b) Contingency table of probabilities between pairs of cell types that are not biological replicates (**Methods**). In both the confusion and contingency matrices, rows correspond to the annotation being conditioned on and sum to unity probability.

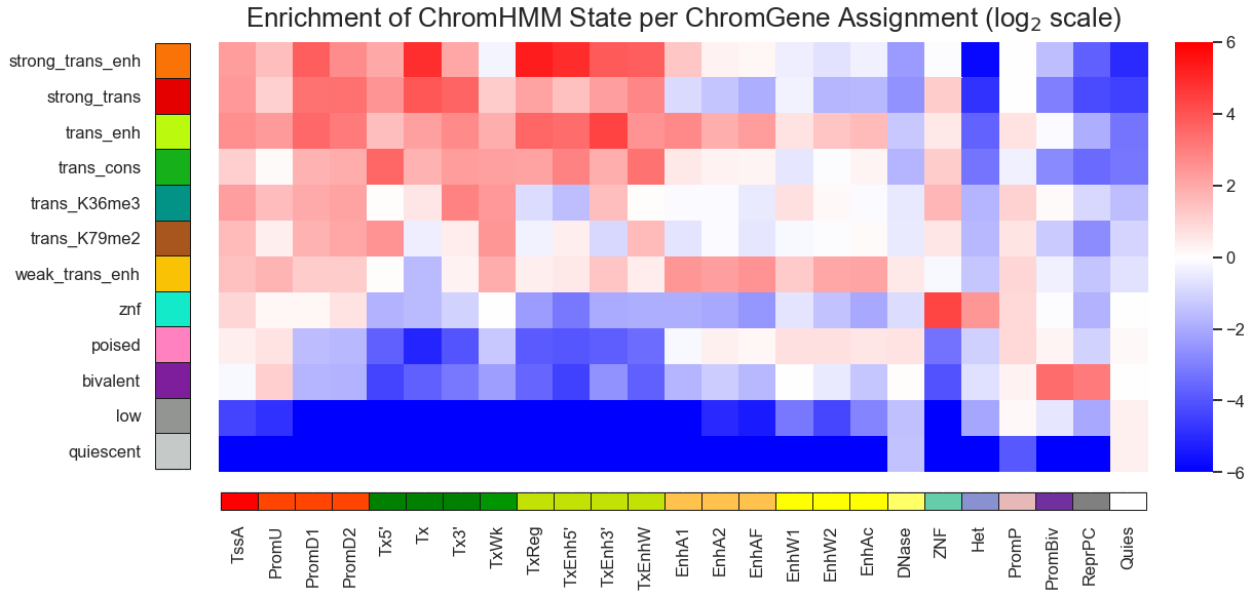

Supplementary Figure 6: Log_2 enrichments of ChromHMM states for each ChromGene assignment

Heatmap where the rows correspond to different ChromGene assignments and the columns to different cell-type specific chromatin states from a previous ChromHMM 25-state model based on the same imputed data [27]. Heatmap values indicate log_2 enrichments for the matched chromatin state annotation in the ChromGene annotation. We set the minimum log_2 enrichment to -6 to prevent washing out of the color scale due to highly negative values.

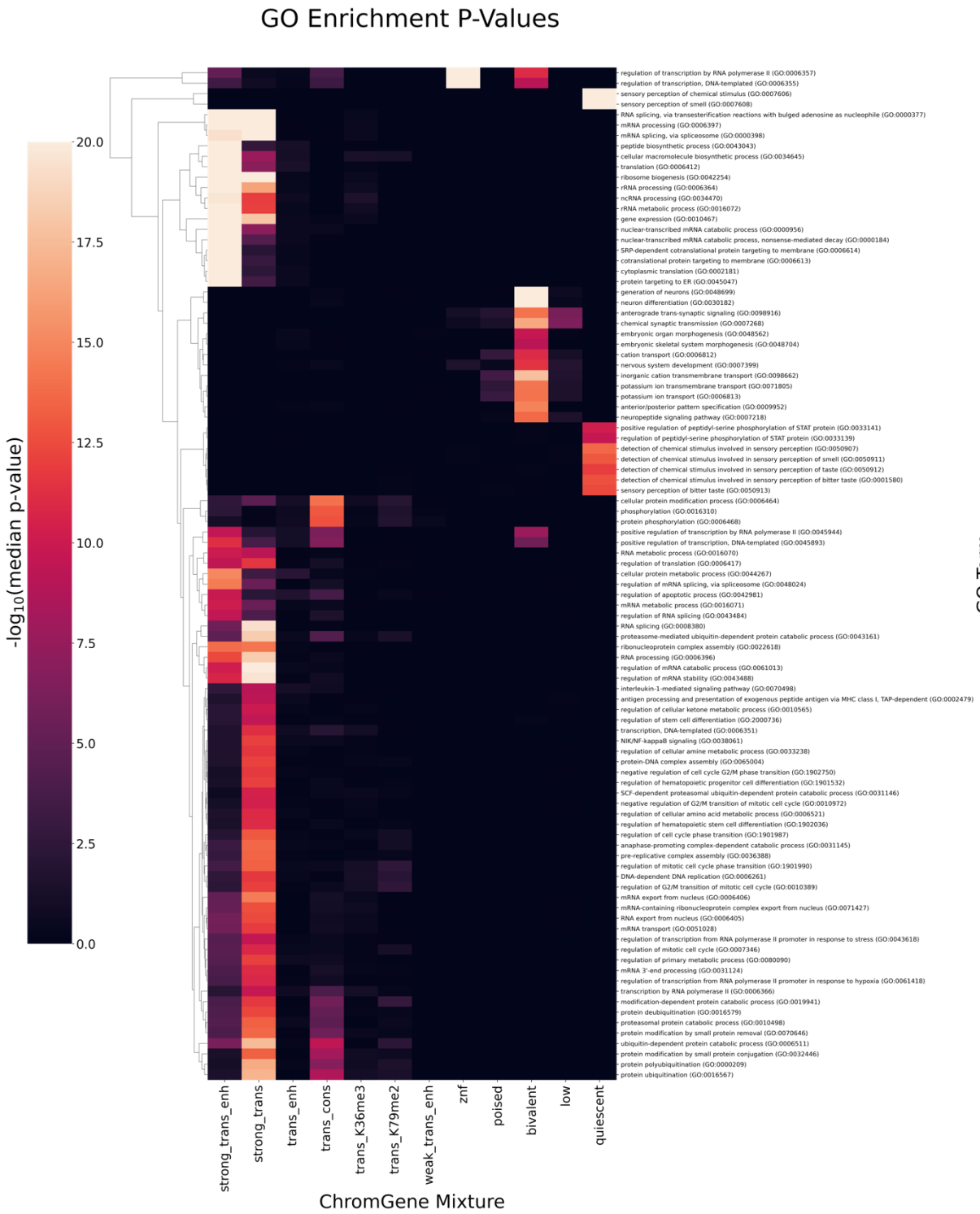

Supplementary Figure 7: Median GO term enrichment across all cell types

Heatmap where the row corresponds to GO terms, columns to ChromGene annotations, and values to the median enrichment $-\log_{10}$(p-value) across all cell types. Rows are filtered so that at least one ChromGene annotation is significant (adjusted p-value < 0.01), and ordered using hierarchical clustering. Maximum $-\log_{10}$(p-value) is set to 20 to prevent washing out of the color scale.

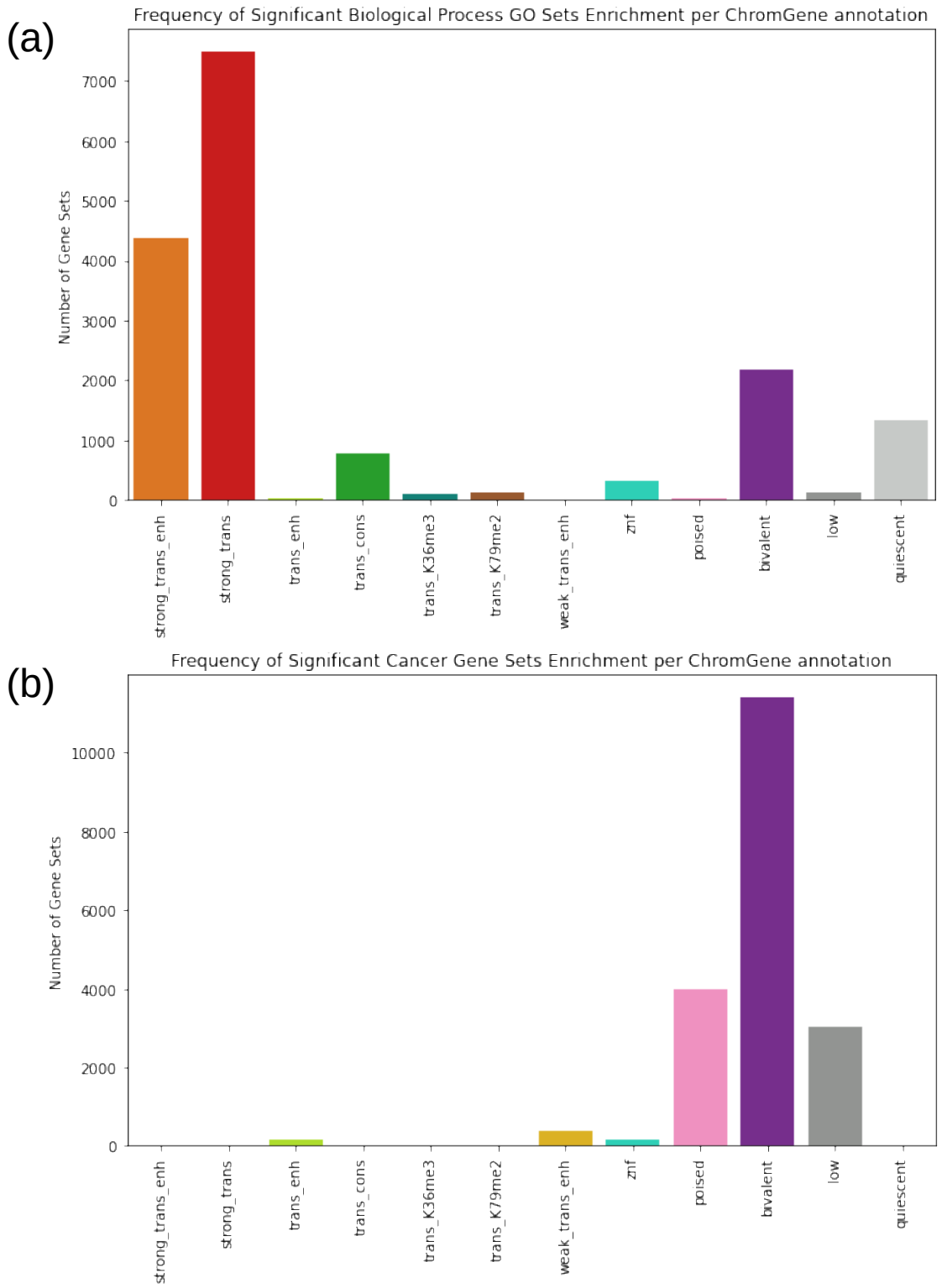

Supplementary Figure 8: Frequency of ChromGene annotations for GO term and cancer gene set enrichments

Count of how often each ChromGene annotations yielded significant p-values ($p < 0.01$, Bonferroni corrected for the number of combinations of cell types (127), mixtures (12), and gene sets) across (a) 6036 gene sets for biological process GO terms and (b) 967 cancer gene sets.

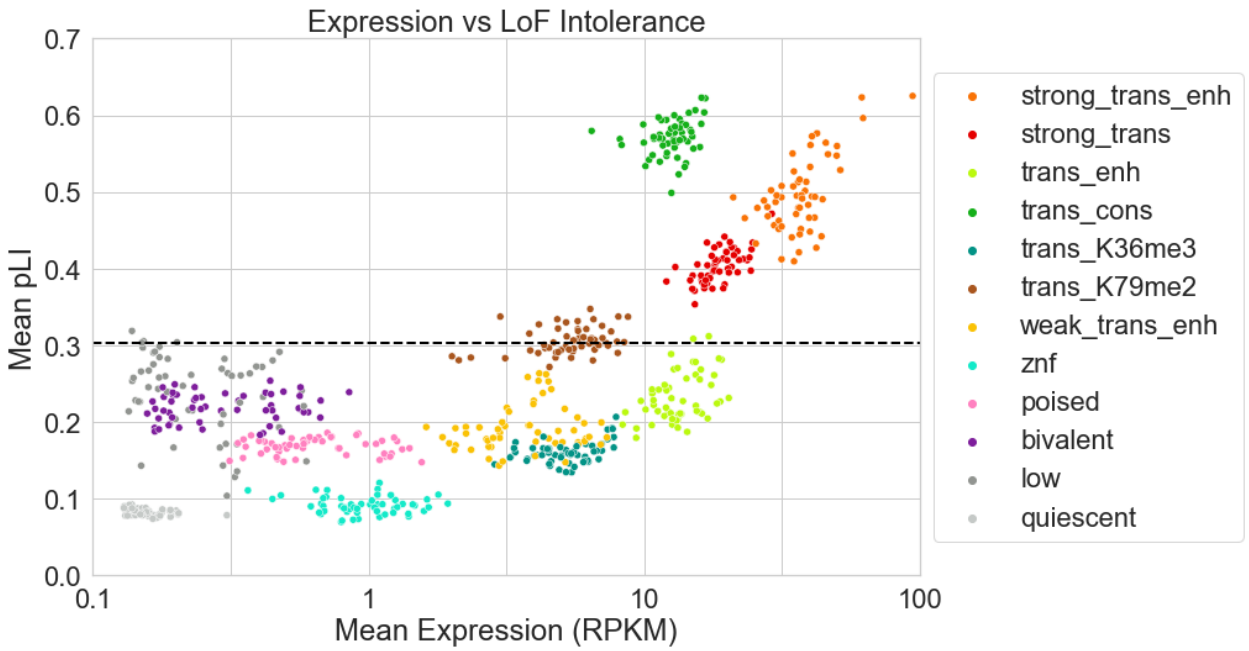

Supplementary Figure 9: Mean pLI vs mean expression

For each cell type and each ChromGene annotation combination, the mean RPKM+0.1 in $\log_{10}$ scale (x-axis) and mean pLI (y-axis) are plotted. Different ChromGene annotations are shown with different colors.

Legends for additional supplementary files

Supplementary Table 1:

Mixture enrichments tab – The columns on this tab after the mixture colors are as follows:

Mnemonic: short identifying name of ChromGene annotation

Description: short description of ChromGene annotation

Overall percentage: percentage of gene-cell type combinations assigned to annotation

Median expression: median expression (RPKM) of genes assigned to annotation across 56 cell types with expression [1]

Median length (kb): median length (kb) of genes assigned to annotation across all cell types, not including flanking regions

Percentage of high-pLI genes (pLI > 0.9): percentage of genes across cell types that have a pLI score > 0.9

Contingency table diagonal / confusion matrix diagonal: percentage consistency of annotations across non-replicate cell types divided by percentage consistency of annotations across replicate cell types

Cell type specificity: 1 - (contingency table diagonal / confusion matrix diagonal), a metric of cell type specificity

Housekeeping gene: gene annotated as housekeeping [35]

Housekeeping gene percentage: percentage of gene-cell type combinations annotated as a housekeeping gene

Housekeeping gene enrichment: fold enrichment of housekeeping genes compared to overall percentage

Housekeeping gene $\log_2$ enrichment: $\log_2$ fold enrichment of housekeeping genes

Housekeeping gene enrichment median enrichment p-value: median p-value of housekeeping gene enrichment across cell types

Constitutively unexpressed gene: gene that has RPKM < 1 across 56 cell types with expression [1]

Constitutively unexpressed gene percentage: percentage of gene-cell type combinations annotated as constitutively unexpressed

Constitutively unexpressed gene enrichment: fold enrichment of constitutively unexpressed genes compared to overall percentage

Constitutively unexpressed gene $\log_2$ enrichment: $\log_2$ fold enrichment of constitutively unexpressed genes

Constitutively unexpressed gene median enrichment p-value: median p-value of constitutively unexpressed gene enrichment across cell types

Constitutively expressed gene: gene that has RPKM > 1 across 56 cell types with expression [1]

Constitutively expressed gene percentage: percentage of gene-cell type combinations annotated as constitutively expressed

Constitutively expressed gene enrichment: fold enrichment of constitutively expressed genes compared to overall percentage

Constitutively expressed gene $\log_2$ enrichment: $\log_2$ fold enrichment of constitutively expressed genes

Constitutively expressed gene median enrichment p-value: median p-value of constitutively expressed gene enrichment across cell types

Olfactory gene: gene annotated as olfactory [30]

Olfactory gene percentage: percentage of gene / cell type combinations annotated as olfactory

Olfactory gene enrichment: fold enrichment of olfactory genes compared to overall percentage

Olfactory gene $\log_2$ enrichment: $\log_2$ fold enrichment of olfactory genes

Olfactory gene median enrichment p-value: median p-value of olfactory gene enrichment across cell types

ZNF gene: gene starts with "ZNF"

ZNF gene percentage: percentage of gene / cell type combinations annotated as ZNF

ZNF gene enrichment: fold enrichment of ZNF genes compared to overall percentage

ZNF gene $\log_2$ enrichment: $\log_2$ fold enrichment of ZNF genes

ZNF gene median enrichment p-value: median p-value of ZNF gene enrichment across cell types

Cancer gene sets enriched (adj $p < 0.01$): the number of cancer gene sets enriched across all cell types for given annotation

Cancer gene sets enriched percentage: the percentage of cancer gene sets enriched across all cell types for given annotation

BP GO terms enriched (adj $p < 0.01$): the number of 'Biological Process' GO term gene sets enriched across all cell types for given annotation

BP GO terms enriched percentage: the percentage of 'Biological Process' GO term gene sets enriched across all cell types for given annotation

Color (hex): hex color for ChromGene annotation

Matplotlib color name: color used in matplotlib for ChromGene annotation [https://xkcd.com/color/rgb/]

State emissions and enrichments tab – The first column gives a color and number for each mixture. The second column gives the mixture mnemonic. The third column gives a number to each individual state of the mixture. The next 12 columns give the emission probabilities for each chromatin mark as indicated. The next two columns gives the maximum and minimum emission probabilities represented as percentages. The next column gives the enrichment of the individual states for annotated TSS. Individual states within each mixture are ordered in decreasing value of this enrichment. The next column gives the initial probability of starting in the state overall. The last column gives the initial probability of the state given the mixture.

Transition Probabilities tab – This tab shows the transition probability indicating the probability when in the state of the row of transitioning to the state of the column. Probabilities are shown for individual states of the model which are ordered and colored based on the mixture to which they belong as indicated.

Supplementary Data: ChromGene annotations

This is a tab delimited file containing the ChromGene annotations for the 127 cell types. Each row after the header row corresponds to one gene. The first five columns from left to right are the chromosome of the gene, the left-most coordinate of the gene, the right-most coordinate of the gene, the gene symbol, and strand of the gene. This is based on hg19 and ENSEMBL v65/GENCODE v10. The remaining columns

correspond to different cell types for which ChromGene annotations are reported as indicated by the names in the header.